Regulation of Store-Operated Ca^{2+} Entry by IP_3 Receptors Independent of Their Ability to Release Ca^{2+}

Pragnya Chakraborty[1,2], Bipan Kumar Deb[1,3], Vikas Arige[5], Thasneem Musthafa[1] Sundeep Malik[5], David I Yule[5], Colin W. Taylor[4,*] and Gaiti Hasan[1,6,*]

[1]National Centre for Biological Sciences, Tata Institute of Fundamental Research, Bellary Road, Bangalore, 560065, India.

[2]SASTRA University, Thanjavur, Tamil Nadu, 613401, India.

[3]Present address: Department of Molecular and Cell Biology, University of California, Berkeley, CA, 94720, USA.

[4]Department of Pharmacology, University of Cambridge, Cambridge, CB2 1PD, UK.

[5]Department of Pharmacology and Physiology, University of Rochester, Rochester, NY, 14642, United States.

[6]Lead Contact

[*]Correspondence: cwt1000@cam.ac.uk, gaiti@ncbs.res.in

ABSTRACT

Loss of endoplasmic reticular (ER) Ca^{2+} activates store-operated Ca^{2+} entry (SOCE) by causing the ER localized Ca^{2+} sensor STIM to unfurl domains that activate Orai channels in the plasma membrane at membrane contact sites (MCS). Here we demonstrate a novel mechanism by which the inositol 1,4,5 trisphosphate receptor (IP_3R), an ER-localized IP_3-gated Ca^{2+} channel, regulates neuronal SOCE. In human neurons, SOCE evoked by pharmacological depletion of ER-Ca^{2+} is attenuated by loss of IP_3Rs, and restored by expression of IP_3Rs even when they cannot release Ca^{2+}, but only if the IP_3Rs can bind IP_3. Imaging studies demonstrate that IP_3Rs enhance association of STIM1 with Orai1 in neuronal cells with empty stores; this requires an IP_3-binding site, but not a pore. Convergent regulation by IP_3Rs, may tune neuronal SOCE to respond selectively to receptors that generate IP_3.

Keywords: Human neural progenitor cell, neuron, IP_3 receptor, Ca^{2+} signaling, STIM Orai, proximity ligation assay, membrane contact site, extended synaptotagmin.

35 **INTRODUCTION**

36 The activities of all eukaryotic cells are regulated by increases in cytosolic free Ca^{2+}
37 concentration ($[Ca^{2+}]_c$), which are almost invariably evoked by the opening of Ca^{2+}-
38 permeable ion channels in biological membranes. The presence of these Ca^{2+}
39 channels within the plasma membrane (PM) and the membranes of intracellular Ca^{2+}
40 stores, most notably the endoplasmic reticulum (ER), allows cells to use both
41 intracellular and extracellular sources of Ca^{2+} to evoke Ca^{2+} signals. In animal cells,
42 the most widely expressed Ca^{2+} signaling sequence links extracellular stimuli, through
43 their specific receptors and activation of phospholipase C, to formation of inositol
44 1,4,5-trisphosphate (IP_3), which then stimulates Ca^{2+} release from the ER through IP_3
45 receptors (IP_3R) (Foskett *et al.*, 2007; Prole and Taylor, 2019). IP_3Rs occupy a central
46 role in Ca^{2+} signaling by releasing Ca^{2+} from the ER. IP_3Rs thereby elicit cytosolic
47 Ca^{2+} signals, and by depleting the ER of Ca^{2+} they initiate a sequence that leads to
48 activation of store-operated Ca^{2+} entry (SOCE) across the PM (Putney, 1986;
49 Thillaiappan *et al.*, 2019). SOCE occurs when loss of Ca^{2+} from the ER causes Ca^{2+} to
50 dissociate from the luminal Ca^{2+}-binding sites of an integral ER protein, stromal
51 interaction molecule 1 (STIM1). STIM1 then unfolds its cytosolic domains to expose a
52 region that binds directly to a Ca^{2+} channel within the PM, Orai, causing it to open and
53 Ca^{2+} to flow into the cell across the PM (Parekh and Putney, 2005; Prakriya and
54 Lewis, 2015; Lewis, 2020). The interactions between STIM1 and Orai occur across a
55 narrow gap between the ER and PM, a membrane contact site (MCS), where STIM1
56 puncta trap Orai channels. While STIM1 and Orai are undoubtedly the core
57 components of SOCE, many additional proteins modulate their interactions (Rosado,

Jenner and Sage, 2000; Palty *et al.*, 2012; Deb, Pathak and Hasan, 2016; Srivats *et al.*, 2016) and other proteins contribute by regulating the assembly of MCS (Chang *et al.*, 2013; Giordano *et al.*, 2013; Kang *et al.*, 2019).

It is accepted that IP_3-evoked Ca^{2+} release from the ER through IP_3Rs is the usual means by which extracellular stimuli evoke SOCE. Here, the role of the IP_3R is widely assumed to be restricted to its ability to mediate Ca^{2+} release from the ER and thereby activate STIM1. Evidence from *Drosophila*, where we suggested an additional role for IP_3Rs in regulating SOCE (Agrawal et al., 2010; Chakraborty et al., 2016), motivated the present study, wherein we examined the contribution of IP_3Rs to SOCE in mammalian neurons. We show that in addition to their ability to activate STIM1 by evoking ER Ca^{2+} release, IP_3Rs also facilitate interactions between active STIM1 and Orai1. This additional role for IP_3Rs, which is regulated by IP_3 but does not require a functional pore, reveals an unexpected link between IP_3, IP_3Rs and Ca^{2+} signaling that is not mediated by IP_3-evoked Ca^{2+} release. We speculate that dual regulation of SOCE by IP_3Rs may allow Ca^{2+} release evoked by IP_3 to be preferentially coupled to SOCE.

RESULTS

Loss of IP_3R1 Attenuates SOCE in Human Neural Stem Cells and Neurons

We investigated the effects of IP_3Rs on SOCE by measuring $[Ca^{2+}]_c$ in human neural stem cells and neurons prepared from embryonic stem cells. Human neural progenitor cells (hNPCs) were derived from H9 embryonic stem cells using small molecules that mimic cues provided during human brain development (Gopurappilly *et al.*, 2018). We

81 confirmed that hNPCs express canonical markers of neural stem cells (**Figure 1A**)
82 and that IP_3R1 is the predominant IP_3R subtype (GEO accession no. GSE109111)
83 (Gopurappilly *et al.*, 2018). An inducible lentiviral shRNA-miR construct targeting
84 IP_3R1 reduced IP_3R1 expression by 93 ± 0.4% relative to a non-silencing (NS)
85 construct (**Figures 1B and 1C**). Carbachol stimulates muscarinic acetylcholine
86 receptors, which are expressed at low levels in hNPCs (Gopurappilly *et al.*, 2018). In
87 Ca^{2+}-free medium, carbachol evoked an increase in $[Ca^{2+}]_c$ in about 10% of hNPCs,
88 consistent with it stimulating Ca^{2+} release from the ER through IP_3Rs. Restoration of
89 extracellular Ca^{2+} then evoked an increase in $[Ca^{2+}]_c$ in all cells that responded to
90 carbachol. Both carbachol-evoked Ca^{2+} release and SOCE were abolished in hNPCs
91 expressing IP_3R1-shRNA, confirming the effectiveness of the IP_3R1 knockdown
92 (**Figure 1- figure supplement 1A-C**).
93 Thapsigargin, a selective and irreversible inhibitor of the ER Ca^{2+} pump
94 (sarcoplasmic/endoplasmic reticulum Ca^{2+}-ATPase, SERCA), was used to deplete the
95 ER of Ca^{2+} and thereby activate SOCE (**Figure 1D**) (Parekh and Putney, 2005).
96 Restoration of extracellular Ca^{2+} to thapsigargin-treated hNPCs evoked a large
97 increase in $[Ca^{2+}]_c$, reflecting the activity of SOCE (**Figure 1D**). The maximal
98 amplitude and rate of SOCE were significantly reduced in cells lacking IP_3R1, but the
99 resting $[Ca^{2+}]_c$ and thapsigargin-evoked Ca^{2+} release were unaffected (**Figures 1D-1F**
100 and **Figure 1- figure supplement 1D and 1E**). STIM1 and Orai1 expression were
101 also unaltered in hNPC lacking IP_3R1 (**Figure 1- figure supplement 1G**). After
102 spontaneous differentiation of hNPC, cells expressed markers typical of mature
103 neurons, and the cells responded to depolarization with an increase in $[Ca^{2+}]_c$ (**Figure**

104 **1- figure supplement 1F and Figure 1- figure supplement 1H-J**). Thapsigargin
105 evoked SOCE in these differentiated neurons; and expression of IP_3R1-shRNA
106 significantly reduced the SOCE response without affecting depolarization-evoked Ca^{2+}
107 signals (**Figures 1H-1J** and **Figure 1- figure supplement 1H-1L**).
108

109 **Loss of IP_3R1 Attenuates SOCE in Human Neuroblastoma Cells**

110 IP_3Rs link physiological stimuli that evoke Ca^{2+} release from the ER to SOCE, but the
111 contribution of IP_3Rs is thought to be limited to their ability to deplete the ER of Ca^{2+}.
112 We have reported that in *Drosophila* neurons there is an additional requirement for
113 IP_3Rs independent of ER Ca^{2+} release (Venkiteswaran and Hasan, 2009; Agrawal *et*
114 *al.*, 2010; Chakraborty *et al.*, 2016). Our results with hNPCs and stem cell-derived
115 neurons suggest a similar requirement for IP_3Rs in regulating SOCE in mammalian
116 neurons. To explore the mechanisms underlying this additional role for IP_3Rs, we
117 turned to a more tractable cell line, SH-SY5Y cells. These cells are derived from a
118 human neuroblastoma; they exhibit many neuronal characteristics (Agholme *et al.*,
119 2010); they express M3 muscarinic acetylcholine receptors that evoke IP_3-mediated
120 Ca^{2+} release and SOCE (Grudt, Usowicz and Henderson, 1996); and they express
121 predominantly IP_3R1 (Wojcikiewicz, 1995; Tovey *et al.*, 2001), with detectable IP_3R3,
122 but no IP_3R2 (**Figure 2A**). We used inducible expression of IP_3R1-shRNA to
123 significantly reduce IP_3R1 expression (by 74 ± 1.2%), without affecting IP_3R3 (**Figures**
124 **2A and 2B**). As expected, carbachol-evoked Ca^{2+} signals in individual SH-SY5Y cells
125 were heterogenous and the carbachol-evoked Ca^{2+} release was significantly reduced
126 by knockdown of IP_3R1 (**Figures 2C and 2D** and **Figure 2 - figure supplement 1A**

127 **and 1B**). Thapsigargin evoked SOCE in SH-SY5Y cells (Grudt, Usowicz and
128 Henderson, 1996), and it was significantly attenuated after knockdown of IP_3R1
129 without affecting resting $[Ca^{2+}]_c$, the Ca^{2+} release evoked by thapsigargin or
130 expression of STIM1 and Orai1 (**Figures 2E-2G** and **Figure 2 - figure supplement**
131 **1C-1E**).

132 We also used CRISPR/Cas9n and Cas9 to disrupt one or both copies of the
133 IP_3R1 gene, subsequently referred to as IKO (one copy knockout) and IKO null (both
134 copies knocked out) in SH-SY5Y cells. IP_3R1 expression was absent in the IKO null
135 (**Figure 2 - figure supplement 1F**) whereas expression of STIM1, STIM2 and Orai1
136 were unperturbed (**Figure 2 - figure supplement 1G**). Carbachol-evoked Ca^{2+}
137 release and thapisgargin-evoked SOCE were significantly reduced (**Figure 2 - figure**
138 **supplement 1H-1J**). Since the IKO null cells were fragile and grew slowly, we
139 examined SOCE in SH-SY5Y cells with disruption of one copy of the IP_3R1 gene. In
140 the IKO cells, IP_3R1 expression, carbachol-evoked Ca^{2+} signals and thapsigargin-
141 evoked SOCE were all reduced (**Figure 2- figure supplement 1K-1Q**).

142 These observations, which replicate those from hNPCs and neurons (**Figure 1**),
143 vindicate our use of SH-SY5Y cells to explore the mechanisms linking IP_3Rs to SOCE
144 in human neurons.

145 Expression of IP_3R1 or IP_3R3 in SH-SY5Y cells expressing IP_3R1-shRNA
146 restored both carbachol-evoked Ca^{2+} release and thapsigargin-evoked SOCE without
147 affecting resting $[Ca^{2+}]_c$ or thapsigargin-evoked Ca^{2+} release (**Figures 2H-2J** and
148 **Figure 2 - figure supplement 2A-2D**). Over-expression of STIM1 in cells expressing
149 NS-shRNA had no effect on SOCE (**Figure 2 - figure supplement 2E and 2F**), but it

150 restored thapsigargin-evoked SOCE in cells expressing IP_3R1-shRNA, without
151 affecting resting $[Ca^{2+}]_c$ or thapsigargin-evoked Ca^{2+} release (**Figures 2K-2M**). We
152 conclude that IP_3Rs are required for optimal SOCE, but they are not essential
153 because additional STIM1 can replace the need for IP_3Rs (**Figure 3A**).
154 It has been reported that SOCE is unaffected by loss of IP_3R in non-neuronal
155 cells (Ma *et al.*, 2001; Chakraborty *et al.*, 2016). Consistent with these observations,
156 the SOCE evoked in HEK cells by stores emptied fully by treatment with thapsigargin
157 was unaffected by expression of IP_3R1 shRNA (**Figure 2 - figure supplement 3A-3C**)
158 or by knockout of all three IP_3R subtypes using CRISPR/cas9 (HEK-TKO cells)
159 (**Figure 2 - figure supplement 3D and 3E**). The association of STIM1 with Orai1 in
160 wild type HEK cells and HEK TKO cells after thapsigargin-evoked store depletion also
161 appeared identical as tested by a proximity ligation assay (PLA, described further in
162 **Figure 5**) (**Figure 2 - figure supplement 3F**). Neuronal and non-neuronal cells may,
163 therefore, differ in the contribution of IP_3R to SOCE. We return to this point later.
164

165 **Binding of IP_3 to IP_3R Without a Functional Pore Stimulates SOCE**

166 IP_3Rs are large tetrameric channels that open when they bind IP_3 and Ca^{2+}, but they
167 also associate with many other proteins (Prole and Taylor, 2019), and many IP_3Rs
168 within cells appear not to release Ca^{2+} (Thillaiappan *et al.*, 2019). A point mutation
169 (D2550A, $IP_3R1^{D/A}$) within the IP_3R1 pore prevents it from conducting Ca^{2+} (Dellis *et*
170 *al.*, 2008). As expected, expression of $IP_3R1^{D/A}$ in cells lacking IP_3R1 failed to rescue
171 carbachol-evoked Ca^{2+} release, but it unexpectedly restored thapsigargin-evoked
172 SOCE (**Figures 3B-3D** and **Figure 3 - figure supplement 1A-E**). We confirmed that

173 rescue of thapsigargin-evoked Ca^{2+} entry by this pore-dead IP_3R was mediated by a
174 conventional SOCE pathway by demonstrating that it was substantially attenuated by
175 siRNA-mediated knockdown of Orai1 (**Figures 3C and 3D** and **Figure 3 - figure**
176 **supplement 1F-1H**).

177 Activation of IP_3Rs is initiated by IP_3 binding to the N-terminal IP_3-binding core of
178 each IP_3R subunit (Prole and Taylor, 2019). Mutation of two conserved phosphate-
179 coordinating residues in the α-domain of the binding core (R568Q and K569Q of
180 IP_3R1, $IP_3R1^{RQ/KQ}$) almost abolishes IP_3 binding (Yoshikawa *et al.*, 1996; Iwai *et al.*,
181 2007), while mutation of a single residue (R568Q, IP_3R1^{RQ}) reduces the IP_3 affinity by
182 ~10-fold (Dellis *et al.*, 2008). Expression of rat $IP_3R1^{RQ/KQ}$ rescued neither carbachol-
183 evoked Ca^{2+} release nor thapsigargin-evoked SOCE in cells lacking IP_3R1 (**Figures**
184 **3E and 3F** and **Figure 3 - figure supplement 1C and 1I)**. However, expression of
185 IP_3R1^{RQ} substantially rescued thapsigargin-evoked SOCE (**Figures 3E and 3F** and
186 **Figure 3 - figure supplement 1J**). Expression of an N-terminal fragment of rat IP_3R
187 (IP_3R1^{1-604}), to which IP_3 binds normally (Iwai *et al.*, 2007), failed to rescue
188 thapsigargin-evoked SOCE (**Figure 3 - figure supplement 1K and 1L)**. These results
189 establish that a functional IP_3-binding site within a full-length IP_3R is required for IP_3Rs
190 to facilitate thapsigargin-evoked SOCE. Hence in cells with empty Ca^{2+} stores, IP_3
191 binding, but not pore-opening, is required for regulation of SOCE by IP_3Rs. In cells
192 stimulated only with thapsigargin and expressing IP_3Rs with deficient IP_3 binding,
193 basal levels of IP_3 are probably insufficient to meet this need.

194 We further examined the need for IP_3 by partially depleting the ER of Ca^{2+} using
195 cyclopiazonic acid (CPA), a reversible inhibitor of SERCA, to allow submaximal

196 activation of SOCE (**Figure 3 - figure supplement 1M and 1N**). Under these
197 conditions, addition of carbachol in Ca^{2+}-free HBSS to SH-SY5Y cells expressing
198 IP_3R1-shRNA caused a small increase in $[Ca^{2+}]_c$ (**Figures 4A-4C**). In the same cells
199 expressing IP_3R1^{DA}, the carbachol-evoked Ca^{2+} release was indistinguishable from
200 that observed in cells without IP_3R^{DA} (**Figures 4B and 4C**), indicating that the small
201 response was entirely mediated by residual native IP_3R1 and/or IP_3R3. Hence, the
202 experiment allows carbachol to stimulate IP_3 production in cells expressing IP_3R1^{DA}
203 without causing additional Ca^{2+} release. The key result is that in cells expressing
204 IP_3R1^{DA}, carbachol substantially increased SOCE (**Figures 4A-4C**). Moreover,
205 addition of carbachol to control shRNA expressing SH-SY5Y cells with maximal store
206 depletion (thapsigargin, Tg, 2μM) also resulted in increased SOCE (**Figure 4 – figure**
207 **supplement 1A**). We conclude that in neuronal cells IP_3, through IP_3Rs, regulates
208 coupling of empty stores to SOCE. This is the first example of an IP_3R mediating a
209 response to IP_3 that does not require the pore of the channel.
210 G-protein-coupled receptors are linked to IP_3 formation through the G-protein
211 Gq, which stimulates phospholipase C β (PLC β). We used YM-254890 to inhibit Gq
212 (Kostenis, Pfeil and Annala, 2020; Patt *et al.*, 2021). As expected, addition of YM-
213 254890 to wild type (WT) or NS-shRNA transfected SH-SY5Y cells abolished the Ca^{2+}
214 signals evoked by carbachol **(Figure 4 - figure supplement 1C)**, but it also reduced
215 the maximal amplitude and rate of thapsigargin-evoked SOCE (**Figures 4D- 4E** and
216 **Figure 3 - figure supplement 1O**). YM-254890 had no effect on the residual
217 thapsigargin-evoked SOCE in SH-SY5Y cells expressing IP_3R1-shRNA **(Figure 4F**
218 and **Figure 3 - figure supplement 1O**). The latter result is important because it

219 demonstrates that the inhibition of SOCE in cells with functional IP_3Rs is not an off-
220 target effect causing a direct inhibition of SOCE.
221 In wild type or HEK-TKO (lacking all three IP_3Rs) cells, YM-254890 had no effect
222 on thapsigargin-evoked SOCE, but it did inhibit SOCE in HEK cells lacking only IP_3R1
223 (**Figures 4G-4I** and **Figure 4 - figure supplement 1D-1G**). These results suggest
224 that in HEK cells, which normally express all three IP_3R subtypes (Mataragka &
225 Taylor, 2018), neither loss of IP_3R1 nor inhibition of Gαq is sufficient on its own to
226 inhibit thapsigargin-evoked SOCE, but when combined there is a synergistic loss of
227 SOCE.
228
229 **IP_3Rs Promote Interaction of STIM1 With Orai1 Within MCS**
230 Our evidence that IP_3Rs intercept coupling between empty stores and SOCE
231 (**Figure 3A**) prompted us to investigate the coupling of STIM1 with Orai1 across the
232 narrow junctions between ER and PM (Carrasco and Meyer, 2011). An *in situ*
233 proximity ligation assay (PLA) is well suited to analyzing this interaction because it
234 provides a signal when two immunolabelled proteins are within ~40 nm of each other
235 (Derangère *et al.*, 2016), a distance comparable to the dimensions of the junctions
236 wherein STIM1 and Orai1 interact (Poteser *et al.*, 2016). We confirmed the specificity
237 of the PLA and demonstrated that it reports increased association of STIM1 with Orai1
238 after treating SH-SY5Y cells with thapsigargin by measuring the surface area of PLA
239 spots (**Figure 5A** and **Figure 5 - figure supplement 1A-1F**) and not the number,
240 because the latter did not change upon store-depletion (**Figure 5 – figure**
241 **supplement 1O**). In cells expressing IP_3R1-shRNA, thapsigargin had no effect on the

242 STIM1-Orai1 interaction reported by PLA, but the interaction was rescued by
243 expression of IP_3R1 or IP_3R1^{DA}. There was no rescue with $IP_3R1^{RQ/KQ}$ (**Figures 5B-**
244 **5E**). WT SH-SY5Y cells that were depleted of basal IP_3 by treatment with the Gq
245 inhibitor YM-254890, showed significantly reduced STIM1-Orai1 interaction after
246 thapsigargin-evoked depletion of Ca^{2+} stores (**Figure 4 - figure supplement 1B**). The
247 results with PLA exactly mirror those from functional analyses (**Figures 1** to **4**),
248 suggesting that IP_3 binding to IP_3R enhances SOCE by facilitating interaction of
249 STIM1 with Orai1 (**Figure 3A**).

250 In independent experiments we tested the effect of fluorescent-tagged and
251 ectopically expressed ligand bound (wild type rat IP_3R1) and mutant (rat $IP_3R1^{RQ/KQ}$;
252 **Figure 6- figure supplement 1A)** IP_3R1 on SOCE dependent STIM1 oligomerization
253 and translocation to ER-PM junctions in SH-SY5Y cells (**Figure 6**). Consistent with
254 previous observations, SOCE did not bring about a measurable change in ER-PM
255 translocation of over-expressed wild type mCherry-IP_3R1 and mCherry-$IP_3R1^{RQ/KQ}$
256 constructs (**Figure 6A-6C**). In agreement with PLA data (**Figure 5)** ER-PM
257 translocation of mVenus-STIM1 upon SOCE induction was reduced significantly in
258 mCherry-$IP_3R1^{RQ/KQ}$ expressing cells compared to mCherry-IP_3R1 expressing SH-
259 SY5Y cells (**Figures 6A, 6B, 6D, and 6E**).

260 Extended synaptotagmins (E-Syts) are ER proteins that stabilize ER-PM
261 junctions including STIM1-Orai1 MCS (Maléth *et al.*, 2014; Kang *et al.*, 2019; Woo *et*
262 *al.*, 2020). Over-expression of E-Syt1 in SH-SY5Y cells expressing IP_3R1-shRNA
263 rescued thapsigargin-evoked Ca^{2+} entry without affecting resting $[Ca^{2+}]_c$ or
264 thapsigargin-evoked Ca^{2+} release (**Figures 7A-7C**). The rescued Ca^{2+} entry is likely to

be mediated by conventional SOCE because it was substantially attenuated by knockdown of STIM1 **(Figures 7D-7F).** Over-expression of E-Syt1 had no effect on SOCE in cells with unperturbed IP_3Rs (**Figures 7G-7I**). These results suggest that attenuated SOCE after loss of IP_3Rs can be restored by exaggerating ER-PM MCS.

DISCUSSION

After identification of STIM1 and Orai1 as core components of SOCE (Prakriya and Lewis, 2015; Thillaiappan *et al.*, 2019), the sole role of IP_3Rs within the SOCE pathway was assumed to be the release of ER Ca^{2+} that triggers STIM1 activation. The assumption is consistent with evidence that thapsigargin-evoked SOCE can occur in avian (Sugawara *et al.*, 1997; Ma *et al.*, 2002; Chakraborty *et al.*, 2016) and mammalian cells without IP_3Rs (Prakriya and Lewis, 2001). Although SOCE in mammalian HEK cells was unaffected by loss of IP_3Rs in our study (**Figure 2- figure supplement 3)**, it was modestly reduced in other studies of mammalian cells (Bartok *et al.*, 2019; Yue *et al.*, 2020). However, additional complexity is suggested by evidence that SOCE may be reduced in cells without IP_3Rs (Chakraborty *et al.*, 2016; Bartok *et al.*, 2019; Yue *et al.*, 2020), by observations implicating phospholipase C in SOCE regulation (Rosado, Jenner and Sage, 2000; Broad *et al.*, 2001), by evidence that SOCE responds differently to IP_3Rs activated by different synthetic ligands (Parekh, Riley and Potter, 2002) and by some, albeit conflicting reports (Woodard *et al.*, 2010; Santoso, Cebotaru and Guggino, 2011; Béliveau, Lessard and Guillemette, 2014; Sampieri *et al.*, 2018; Ahmad *et al.*, 2022), that IP_3Rs may interact with STIM

287 and/or Orai (Woodard *et al.*, 2010; Santoso, Cebotaru and Guggino, 2011; Béliveau,
288 Lessard and Guillemette, 2014; Sampieri *et al.*, 2018).

289 We identified two roles for IP_3Rs in controlling endogenous SOCE in human
290 neurons. As widely reported, IP_3Rs activate STIM1 by releasing Ca^{2+} from the ER, but
291 they also, and independent of their ability to release Ca^{2+}, enhance interactions
292 between active STIM1 and Orai1 (**Figure 8**). The second role for IP_3Rs can be
293 supplanted by over-expressing other components of the SOCE complex, notably
294 STIM1 or ESyt1 (**Figures 2K-2M** and **Figures 7A and 7B**). It is intriguing that STIM1
295 (Carrasco and Meyer, 2011; Lewis, 2020), ESyt1 (Giordano *et al.*, 2013) and perhaps
296 IP_3Rs (through the IP_3-binding core) interact with phosphatidylinositol 4,5-
297 bisphosphate (PIP_2), which is dynamically associated with SOCE-MCS (Kang *et al.*,
298 2019). We suggest that the extent to which IP_3Rs tune SOCE in different cells is
299 probably determined by the strength of Gq signaling and endogenous interactions
300 between STIM1 and Orai1. The latter is likely to depend on the relative expression of
301 STIM1 and Orai1 (Woo *et al.*, 2020), the STIM isoforms expressed, expression of
302 proteins that stabilize STIM1-Orai1 interactions (Darbellay *et al.*, 2011; Rana *et al.*,
303 2015; Rosado *et al.*, 2016; Knapp *et al.*, 2022), and the size and number of the MCS
304 where STIM1 and Orai1 interact (Kang *et al.*, 2019). The multifarious contributors to
305 SOCE suggest that cells may differ in whether they express “spare capacity”. In
306 neuronal cells, loss of IP_3 (**Figure 4D**) or of the dominant IP_3R isoform (IP_3R1-shRNA;
307 **Figures 1 and 2**) is sufficient to unveil the contribution of IP_3R to SOCE, whereas
308 HEK cells require loss of both IP_3 and IP_3R1 to unveil the contribution (**Figures 4H**
309 **and 4I**). The persistence of SOCE in cells devoid of IP_3Rs (**Figure 2 - figure**

310 **supplement 3D and 3E**) (Prakriya and Lewis, 2001; Ma *et al.*, 2002) probably arises
311 from adaptive changes within the SOCE pathway. This does not detract from our
312 conclusion that under physiological conditions, where receptors through IP_3 initiate
313 SOCE, IP_3Rs actively regulate SOCE.

314 The IP_3Rs that initiate Ca^{2+} signals reside in ER immediately beneath the PM and
315 alongside, but not within, the MCS where STIM1 accumulates after store depletion
316 (Thillaiappan *et al.*, 2017; **Figure 6A and 6B**). In migrating cells too, IP_3Rs and STIM1
317 remain separated as they redistribute to the leading edge (Okeke *et al.*, 2016).
318 Furthermore, there is evidence that neither STIM1 nor STIM2 co-immmunoprecipitate
319 with IP_3R1 (Ahmad *et al.*, 2022). We suggest, and consistent with evidence that
320 SOCE in cells without IP_3Rs can be restored by over-expressing E-Syt1 (**Figures 7A-**
321 **7C**), that ligand-bound IP_3Rs probably facilitate SOCE by stabilizing the MCS wherein
322 STIM1 and Orai1 interact, rather than by directly regulating either protein. This
323 proposal provides an analogy with similar structural roles for IP_3Rs in maintaining
324 MCS between ER and mitochondria (Bartok *et al.*, 2019) or lysosomes (Atakpa *et al.*,
325 2018) (**Figure 8**). Since both contributions of IP_3Rs to SOCE require IP_3 binding
326 (**Figures 3E and 3F**), each is ultimately controlled by receptors that stimulate IP_3
327 formation (**Figures 4B and 4C**). Convergent regulation by IP_3Rs at two steps in the
328 SOCE pathway may ensure that receptor-regulated PLC activity provides the most
329 effective stimulus for SOCE; more effective, for example, than ryanodine receptors,
330 which are also expressed in neurons (**Figure 8B**). By opening IP_3Rs parked alongside
331 SOCE MCS (Thillaiappan *et al.*, 2017; Ahmad *et al.*, 2022), IP_3 selectively releases

332 Ca^{2+} from ER that is optimally placed to stimulate SOCE, and by facilitating Orai1-
333 STIM1 interactions IP_3 reinforces this local activation of SOCE (**Figure 8A and 8B**).
334 We conclude that IP_3-regulated IP_3Rs regulate SOCE by mediating Ca^{2+} release
335 from the ER, thereby activating STIM1 and/or STIM2 (Ahmad *et al.*, 2022) and,
336 independent of their ability to release Ca^{2+}, IP_3Rs facilitate the interactions between
337 STIM and Orai that activate SOCE. Dual regulation of SOCE by IP_3 and IP_3Rs allows
338 robust control by cell-surface receptors and may reinforce local stimulation of Ca^{2+}
339 entry.
340

341 **ACKNOWLEDGEMENTS**

342 This research was supported by grants to G.H. from the Dept. of Biotechnology, Govt.
343 of India (BT/PR6371/COE/34/19/2013) and NCBS-TIFR core support, to C.W.T. from
344 the Wellcome Trust (101844) and Biotechnology and Biological Sciences Research
345 Council (BB/T012986/1) and to D.I.Y from the NIH (NIDCR, DE014756). P.C is
346 supported by a DST-INSPIRE fellowship (DST/INSPIRE Fellowship/2017/IF170360)
347 and she received an Infosys-NCBS travel award to visit C.W.T.'s lab at Cambridge.
348 We are grateful to Renjitha Gopurappilly (NCBS, TIFR) for the derivation of human
349 neural precursor cells. We acknowledge use of the Central Imaging and Flow
350 Cytometry Facility (CIFF), Stem Cell Culture Facility and Biosafety level-2 laboratory
351 facility at NCBS, TIFR.
352

353 **DISCLOSURE AND COMPETING INTEREST STATEMENT**

354 The authors declare no competing interests.

REFERENCES

Agholme, L., Lindström, T., Kågedal, K., Marcusson, J. and Hallbeck, M. 2010. An in vitro model for neuroscience: differentiation of SH-SY5Y cells into cells with morphological and biochemical characteristics of mature neurons. *J. Alzheimer's Dis.* 20:1069–1082.

Agrawal, N., Venkiteswaran, G., Sadaf, S., Padmanabhan, N., Banerjee, S. and Hasan, G. 2010. Inositol 1, 4, 5-trisphosphate receptor and dSTIM function in *Drosophila* insulin-producing neurons regulates systemic intracellular calcium homeostasis and flight. *J. Neurosci*. 30:1301-1313.

Ahmad, M. et al. 2022. Functional communication between IP_3R and STIM2 at subthreshold stimuli is a critical checkpoint for initiation of SOCE. *Proc. Natl. Acad. Sci.* 119: e2114928118.

Atakpa, P., Thillaiappan, N.B., Mataragka, S., Prole, D.L. and Taylor, C.W. 2018. IP_3 receptors preferentially associate with ER-lysosome contact sites and selectively deliver Ca^{2+} to lysosomes. *Cell Rep.* 25:3180-3193.

Auyeung, V.C., Ulitsky, I., McGeary, S.E. and Bartel, D.P. 2013. Beyond secondary structure: primary-sequence determinants license pri-miRNA hairpins for processing. *Cell.* 152:844-858.

Bartok, A., Weaver, D., Golenár, T., Nichtova, Z., Katona, M., Bánsághi, S., Alzayady, K.J., Thomas, V.K., Ando, H., Mikoshiba, K. and Joseph, S.K. 2019. IP_3 receptor isoforms differently regulate ER-mitochondrial contacts and local calcium transfer. *Nat. Commun*. 10:1-14.

378 Béliveau, É., Lessard, V. and Guillemette, G. 2014. STIM1 positively regulates the
379 Ca^{2+} release activity of the inositol 1,4,5-trisphosphate receptor in bovine aortic
380 endothelial cells. *PLoS One.* 9: e114718.
381 Broad, L.M., Braun, F.J., Lievremont, J.P., Bird, G.S.J., Kurosaki, T. and Putney Jr,
382 J.W. 2001. Role of the phospholipase C-inositol 1, 4, 5-trisphosphate pathway in
383 calcium release-activated calcium current and capacitative calcium entry. *J. Biol.*
384 *Chem.* 276:15945–15952.
385 Carrasco, S. and Meyer, T. 2011. STIM proteins and the endoplasmic reticulum-
386 plasma membrane junctions. *Annu. Rev. Biochem.* 80:973–1000.
387 Chakraborty, S., Deb, B.K., Chorna, T., Konieczny, V., Taylor, C.W. and Hasan, G.
388 2016. Mutant IP_3 receptors attenuate store-operated Ca^{2+} entry by destabilizing
389 STIM–Orai interactions in *Drosophila* neurons. *J. Cell Sci.* 129:3903–3910.
390 Chang, C.L., Hsieh, T.S., Yang, T.T., Rothberg, K.G., Azizoglu, D.B., Volk, E., Liao,
391 J.C. and Liou, J. 2013. Feedback regulation of receptor-induced Ca^{2+} signaling
392 mediated by E-Syt1 and Nir2 at endoplasmic reticulum-plasma membrane
393 junctions. *Cell Rep*. 5:813–825.
394 Darbellay, B., Arnaudeau, S., Bader, C.R., Konig, S. and Bernheim, L. 2011. STIM1L
395 is a new actin-binding splice variant involved in fast repetitive Ca^{2+} release. *J.*
396 *Cell Biol.* 194:335-346.
397 Deb, B. K., Pathak, T. and Hasan, G. 2016. Store-independent modulation of Ca^{2+}
398 entry through Orai by Septin 7. *Nat. Commun.* 7:1-15.
399 Dellis, O., Rossi, A.M., Dedos, S.G. and Taylor, C.W. 2008. Counting functional
400 inositol 1, 4, 5-trisphosphate receptors into the plasma membrane. *J Biol. Chem.*

283:751-755.

Derangère, V., Bruchard, M., Végran, F. and Ghiringhelli, F. 2016. Proximity Ligation Assay (PLA) protocol using Duolink® for T cells. *Bio-protocol.* 6:e1811.

Forostyak, O., Romanyuk, N., Verkhratsky, A., Sykova, E. and Dayanithi, G. 2013. Plasticity of calcium signaling cascades in human embryonic stem cell-derived neural precursors. *Stem Cells Dev.* 22:1506-1521.

Foskett, J.K., White, C., Cheung, K.H. and Mak, D.O.D. 2007. Inositol trisphosphate receptor Ca^{2+} release channels. *Physiol. Rev.* 87:593–658.

Giordano, F., Saheki, Y., Idevall-Hagren, O., Colombo, S.F., Pirruccello, M., Milosevic, I., Gracheva, E.O., Bagriantsev, S.N., Borgese, N. and De Camilli, P. 2013. PI(4, 5) P_2-dependent and Ca^{2+}-regulated ER-PM interactions mediated by the extended synaptotagmins. *Cell*. 153:1494-1509.

Gopurappilly, R., Deb, B.K., Chakraborty, P. and Hasan, G. 2018. Stable STIM1 knockdown in self-renewing human neural precursors promotes premature neural differentiation. *Front. Mol. Neurosci.* 11:178.

Grudt, T. J., Usowicz, M. M. and Henderson, G. 1996. Ca^{2+} entry following store depletion in SH-SY5Y neuroblastoma cells. *Mol. Brain Res.* 36:93–100.

Grynkiewicz, G., Poenie, M. and Tsien, R. Y. 1985. A new generation of Ca^{2+} indicators with greatly improved fluorescence properties. *J. Biol. Chem.* 260:3440–3450.

Iwai, M., Michikawa, T., Bosanac, I., Ikura, M. and Mikoshiba, K. 2007. Molecular basis of the isoform-specific ligand-binding affinity of inositol 1, 4, 5-trisphosphate receptors. *J. Biol. Chem.* 282:12755–12764.

Kang, F., Zhou, M., Huang, X., Fan, J., Wei, L., Boulanger, J., Liu, Z., Salamero, J., Liu, Y. and Chen, L. 2019. E-syt1 Re-arranges STIM1 clusters to stabilize ring-shaped ER-PM contact sites and accelerate Ca^{2+} store replenishment. *Sci Rep.* 9:1-11.

Knapp, M.L., Alansary, D., Poth, V., Förderer, K., Sommer, F., Zimmer, D., Schwarz, Y., Künzel, N., Kless, A., Machaca, K. and Helms, V., 2022. A longer isoform of Stim1 is a negative SOCE regulator but increases cAMP-modulated NFAT signaling. *EMBO reports*, *23:* e53135.

Knott, S.R., Maceli, A.R., Erard, N., Chang, K., Marran, K., Zhou, X., Gordon, A., El Demerdash, O., Wagenblast, E., Kim, S. and Fellmann, C. 2014. A computational algorithm to predict shRNA potency. *Mol. Cell.* 56:796-807.

Lewis, R. S. 2020. Store-operated calcium channels: From function to structure and back again. *Cold Spring Harb. Perspect. Biol.* 12: a035055.

Ma, H. T., Venkatachalam, K., Li, H. S., Montell, C., Kurosaki, T., Patterson, R. L., & Gill, D. L. 2001. Assessment of the role of the inositol 1,4,5-trisphosphate receptor in the activation of transient receptor potential channels and store-operated Ca^{2+} entry channels. *J Biol Chem*, 276: 18888–18896.

Ma, H. T., Venkatachalam, K., Parys, J. B., & Gill, D. L. 2002. Modification of store-operated channel coupling and inositol trisphosphate receptor function by 2-aminoethoxydiphenyl borate in DT40 lymphocytes. *J Biol Chem*, 277: 6915–6922.

Maléth, J., Choi, S., Muallem, S. and Ahuja, M. 2014. Translocation between PI(4, 5)P_2-poor and PI(4, 5)P_2-rich microdomains during store depletion determines

STIM1 conformation and Orai1 gating. *Nat Commun.* 5:1–10.

Mataragka, S. and Taylor, C. W. 2018. All three IP_3 receptor subtypes generate Ca^{2+} puffs, the universal building blocks of IP_3-evoked Ca^{2+} signals. *J Cell Sci.* 131: jcs220848.

Miotke, L., Lau, B. T., Rumma, R. T., & Ji, H. P. 2014. High sensitivity detection and quantitation of DNA copy number and single nucleotide variants with single color droplet digital PCR. *Anal. Chem.*, *86:* 2618-2624.

Nunes-Hasler, P., Maschalidi, S., Lippens, C., Castelbou, C., Bouvet, S., Guido, D., Bermont, F., Bassoy, E.Y., Page, N., Merkler, D. and Hugues, S. 2017. STIM1 promotes migration, phagosomal maturation and antigen cross-presentation in dendritic cells. *Nat Commun*. 8:1-15.

Okeke, E., Parker, T., Dingsdale, H., Concannon, M., Awais, M., Voronina, S., Molgó, J., Begg, M., Metcalf, D., Knight, A.E. and Sutton, R. 2016. Epithelial–mesenchymal transition, IP_3 receptors and ER–PM junctions: Translocation of Ca^{2+} signalling complexes and regulation of migration. *Biochem. J*. 473:757–767.

Palty, R., Raveh, A., Kaminsky, I., Meller, R. and Reuveny, E. 2012. SARAF inactivates the store operated calcium entry machinery to prevent excess calcium refilling. *Cell*. 149:425-438.

Parekh, A. B. and Putney, J. W. 2005. Store-operated calcium channels. *Physiol. Rev.* 85:757–810.

Parekh, A. B., Riley, A. M. and Potter, B. V. L. 2002. Adenophostin A and ribophostin, but not inositol 1,4,5-trisphosphate or manno-adenophostin, activate the Ca^{2+} release-activated Ca^{2+} current, ICRAC, in weak intracellular Ca^{2+} buffer.

Biochem. J. 361:133–141.

Patt, J., Alenfelder, J., Pfeil, E.M., Voss, J.H., Merten, N., Eryilmaz, F., Heycke, N., Rick, U., Inoue, A., Kehraus, S. and Deupi, X. 2021. An experimental strategy to probe Gq contribution to signal transduction in living cells. *J. Biol. Chem.* 296:100472.

Poteser, M., Leitinger, G., Pritz, E., Platzer, D., Frischauf, I., Romanin, C. and Groschner, K. 2016. Live-cell imaging of ER-PM contact architecture by a novel TIRFM approach reveals extension of junctions in response to store-operated Ca^{2+}-entry. *Sci. Rep*. 6:1-13.

Prakriya, M. and Lewis, R. S. 2001. Potentiation and inhibition of Ca^{2+} release-activated Ca^{2+} channels by 2-aminoethyldiphenyl borate (2-APB) occurs independently of IP_3 receptors. *J Physiol*. 536:3–19.

Prakriya, M. and Lewis, R. S. 2015. Store-operated calcium channels pharmacology. *Physiol. Rev.* 307:1383–1436.

Prole, D. L. and Taylor, C. W. 2019. Structure and function of IP_3 receptors. *Cold Spring Harb. Perspect. Biol.* 11: a035063.

Putney, J. W. 1986. A model for receptor-regulated calcium entry. *Cell Calcium*. 7:1–12.

Ran, F. A., Hsu, P. D., Wright, J., Agarwala, V., Scott, D. A., & Zhang, F. 2013. Genome engineering using the CRISPR-Cas9 system. *Nat. Protoc*. 8: 2281-2308.

Rana, A., Yen, M., Sadaghiani, A.M., Malmersjö, S., Park, C.Y., Dolmetsch, R.E. and Lewis, R.S. 2015. Alternative splicing converts STIM2 from an activator to an

493 inhibitor of store-operated calcium channels. *J Cell Biol.* 209: 653-670.
494 Reinhardt, P., Glatza, M., Hemmer, K., Tsytsyura, Y., Thiel, C.S., Höing, S., Moritz, S.,
495 Parga, J.A., Wagner, L., Bruder, J.M. and Wu, G. 2013. Derivation and
496 expansion using only small molecules of human neural progenitors for
497 neurodegenerative disease modeling. *PLoS One.* 8: e59252.
498 Rosado, J.A., Diez, R., Smani, T. and Jardín, I. 2016. STIM and Orai1 variants in
499 store-operated calcium entry. *Front. Pharmacol.* 6:325.
500 Rosado, J. A., Jenner, S. and Sage, S. O. 2000. A role for the actin cytoskeleton in
501 the initiation and maintenance of store-mediated calcium entry in human
502 platelets. Evidence for conformational coupling. *J Biol. Chem*. 275: 7527–7533.
503 Saleem, H., Tovey, S.C., Rahman, T., Riley, A.M., Potter, B.V. and Taylor, C.W. 2013.
504 Stimulation of inositol 1, 4, 5-trisphosphate (IP_3) receptor subtypes by analogues
505 of IP_3. *PLoS One.* 8:e54877.
506 Sampieri, A., Santoyo, K., Asanov, A. and Vaca, L. 2018. Association of the IP_3R to
507 STIM1 provides a reduced intraluminal calcium microenvironment, resulting in
508 enhanced store-operated calcium entry. *Sci Rep*. 8:1–13.
509 Santoso, N. G., Cebotaru, L. and Guggino, W. B. 2011. Polycystin-1, 2, and STIM1
510 interact with IP_3R to modulate ER Ca^{2+} release through the PI3K/Akt pathway.
511 *Cell Physiol Biochem*. 27:715–726.
512 Srivats, S., Balasuriya, D., Pasche, M., Vistal, G., Edwardson, J.M., Taylor, C.W. and
513 Murrell-Lagnado, R.D. 2016. Sigma-1 receptors inhibit store-operated Ca^{2+} entry
514 by attenuating coupling of STIM1 to Orai1. *J. Cell Biol.* 213: 65–79.
515 Sugawara, H., Kurosaki, M., Takata, M. and Kurosaki, T. 1997. Genetic evidence for

516 involvement of type 1, type 2 and type 3 inositol 1, 4, 5-trisphosphate receptors
517 in signal transduction through the B-cell antigen receptor. *EMBO J*. 16:3078–
518 3088.
519 Thillaiappan, N.B., Chavda, A.P., Tovey, S.C., Prole, D.L. and Taylor, C.W. 2017.
520 Ca^{2+} signals initiate at immobile IP_3 receptors adjacent to ER-plasma membrane
521 junctions. *Nat. Commun.* 8:1-16.
522 Thillaiappan, N.B., Chakraborty, P., Hasan, G. and Taylor, C.W. 2019. IP_3 receptors
523 and Ca^{2+} entry. *Biochim Biophys Acta Mol Cell Res*. 1866:1092–1100.
524 Tovey, S.C., De Smet, P., Lipp, P., Thomas, D., Young, K.W., Missiaen, L., De Smedt,
525 H., Parys, J.B., Berridge, M.J., Thuring, J. and Holmes, A. 2001. Calcium puffs
526 are generic $InsP_3$-activated elementary calcium signals and are downregulated
527 by prolonged hormonal stimulation to inhibit cellular calcium responses. *J. Cell*
528 *Sci*. 114:3979-3989.
529 Venkiteswaran, G. and Hasan, G. 2009. Intracellular Ca^{2+} signaling and store-
530 operated Ca^{2+} entry are required in *Drosophila* neurons for flight. *Proc. Natl.*
531 *Acad. Sci. U. S. A.* 106:10326–10331.
532 Wojcikiewicz, R. J. H. 1995. Type I, II, and III inositol 1,4,5-trisphosphate receptors
533 are unequally susceptible to down-regulation and are expressed in markedly
534 different proportions in different cell types. *J. Biol. Chem*. 270:11678–11683.
535 Woo, J.S., Sun, Z., Srikanth, S. and Gwack, Y. 2020. The short isoform of extended
536 synaptotagmin-2 controls Ca^{2+} dynamics in T cells via interaction with STIM1.
537 *Sci. Rep*. 10:1-13.
538 Woodard, G.E., López, J.J., Jardín, I., Salido, G.M. and Rosado, J.A. 2010. TRPC3

539 regulates agonist-stimulated Ca^{2+} mobilization by mediating the interaction
540 between type I inositol 1, 4, 5-trisphosphate receptor, RACK1, and Orai1. *J. Biol.*
541 *Chem*. 285: 8045–8053.
542 Yoshikawa, F., Morita, M., Monkawa, T., Michikawa, T., Furuichi, T. and Mikoshiba, K.
543 1996. Mutational analysis of the ligand binding site of the inositol 1, 4, 5-
544 trisphosphate receptor. *J. Biol. Chem.* 271:18277-18284.
545 Yue, L., Wang, L., Du, Y., Zhang, W., Hamada, K., Matsumoto, Y., Jin, X., Zhou, Y.,
546 Mikoshiba, K., Gill, D.L. and Han, S. 2020. Type 3 inositol 1, 4, 5-trisphosphate
547 receptor is a crucial regulator of calcium dynamics mediated by endoplasmic
548 reticulum in HEK cells. *Cells*. 9:275.

549 **Figure 1. Loss of IP_3R1 Attenuates SOCE in Human Neural Stem Cells**

550 (**A**) Confocal images of hNPCs (passage 6) stained for DAPI and neural stem cell

551 proteins: Pax6 and Ki67 (proliferation marker). Scale bars, 50 μm.

552 (**B**) WB for IP_3R1 of hNPCs expressing non-silencing (NS) or IP_3R1-shRNA.

553 (**C**) Summary results (mean ± s.d., n = 3) show IP_3R1 expression relative to actin. $^{**}P$

554 < 0.01, Student's t-test with unequal variances.

555 (**D**) Changes in $[Ca^{2+}]_c$ evoked by thapsigargin (Tg, 10 μM) in Ca^{2+}-free HBSS and

556 then restoration of extracellular Ca^{2+} (2 mM) in hNPCs expressing NS or IP_3R1-

557 shRNA. Mean ± s.e.m. from 3 independent experiments, each with 4 replicates that

558 together included 100-254 cells. Inset shows the target of Tg.

559 (**E-G**) Summary results (individual cells, median (bar), 25th and 75th percentiles (box)

560 and mean (circle)) show Ca^{2+} signals evoked by Tg or Ca^{2+} restoration (**E**), rate of

561 Ca^{2+} entry (**F**) and resting $[Ca^{2+}]_c$ (**G**). $^{***}P$ < 0.001, Mann-Whitney U-test.

562 (**H**) Changes in $[Ca^{2+}]_c$ evoked by Tg (10 μM) in Ca^{2+}-free HBSS and after restoring

563 extracellular Ca^{2+} (2 mM) in neurons (differentiated hNPCs) expressing NS or IP_3R1-

564 shRNA. Mean ± s.e.m. from 3 experiments with ~200 cells.

565 (**I,J**) Summary results (presented as in E-G) show Ca^{2+} signals evoked by Tg or Ca^{2+}

566 restoration (**I**) and rate of Ca^{2+} entry (**J**). $^{***}P$ < 0.001. Mann-Whitney U-test.

567 See also **Figure 1 - figure supplement 1.**

568 **Source data in Figure 1 source data file**

569 **Figure 2. Loss of IP_3R1 Attenuates SOCE in SH-SY5Y Cells**

570 (**A**) WB for IP_3R1-3 of SH-SY5Y cells expressing non-silencing (NS) or IP_3R1-shRNA.

571 (**B**) Summary results (mean ± s.d., n = 4) show IP_3R expression relative to actin

572 normalized to control NS cells. $^{**}P < 0.01$, Student's t-test with unequal variances.

573 (**C**) Ca^{2+} signals evoked by carbachol (CCh, 3 μM) in SH-SY5Y cells expressing NS or

574 IP_3R1-shRNA. Mean ± s.e.m. from 3 experiments with 70-90 cells.

575 (**D**) Summary results show peak changes in $[Ca^{2+}]_c$ ($\Delta[Ca^{2+}]_c$) evoked by CCh. $^{***}P <$

576 0.001, Mann-Whitney U-test.

577 (**E**) Ca^{2+} signals evoked by thapsigargin (Tg, 10 μM) in Ca^{2+}-free HBSS and then after

578 restoration of extracellular Ca^{2+} (2 mM) in cells expressing NS or IP_3R1-shRNA. Mean

579 ± s.e.m. from 3 experiments with ~50 cells.

580 (**F, G**) Summary results (individual cells, mean ± s.e.m., n = 3, ~50 cells) show peak

581 changes in $[Ca^{2+}]_c$ evoked by Ca^{2+} restoration ($\Delta[Ca^{2+}]_c$) (**F**) and rate of Ca^{2+} entry (**G**).

582 $^{***}P < 0.001$, Mann-Whitney U-test.

583 (**H**) Ca^{2+} signals evoked by Tg and then Ca^{2+} restoration in cells expressing NS-

584 shRNA, or IP_3R1-shRNA alone or with IP_3R1 or IP_3R3. Traces show mean ± s.e.m.

585 (50-115 cells from 3 experiments).

586 (**I, J**) Summary results (mean ± s.e.m, 50-115 cells from 3 experiments) show peak

587 increases in $[Ca^{2+}]_c$ ($\Delta[Ca^{2+}]_c$) evoked by Ca^{2+} restoration (**I**) and rates of Ca^{2+} entry

588 (**J**) evoked by restoring extracellular Ca^{2+}.

589 (**K**) Effects of thapsigargin (Tg, 10 μM) in Ca^{2+}-free HBSS and then after Ca^{2+}

590 restoration (2 mM) in cells expressing IP_3R1-shRNA alone or with IP_3R1 or mCh-

591 STIM1. Traces show mean ± s.e.m. (100-150 cells from 3 experiments).

592 (**L, M**) Summary results (mean ± s.e.m.) show peak increase in $[Ca^{2+}]_c$ after Ca^{2+}

593 restoration ($\Delta[Ca^{2+}]_c$) (**L**) and rate of Ca^{2+} entry (**M**). Different letters indicate

594 significant differences (panels I, J, L, M), $P < 0.001$, one-way ANOVA with pair-wise

595 Tukey's test.

596 See also **Figure 2 with 3 supplements (Figure 2 - figure supplements 1 - 3).**

597 **Source data in Figure 2 source data file**

598 **Figure 3. Regulation of SOCE by IP_3R Requires IP_3 Binding but Not a Functional**
599 **Pore in SH-SY5Y cells**

600 (**A**) SOCE is activated when loss of Ca^{2+} from the ER through IP_3Rs activates STIM1
601 (i). Our results suggest an additional role for IP_3Rs (ii).

602 (**B**) SH-SY5Y cells expressing IP_3R1-shRNA alone or with IP_3R1 or IP_3R1^{DA} were
603 stimulated with thapsigargin (Tg, 1 μM) in Ca^{2+}-free HBSS before restoring
604 extracellular Ca^{2+} (2 mM). Traces show mean ± s.e.m, for 100-150 cells from 3
605 experiments.

606 (**C**) Cells expressing IP_3R1-shRNA and IP_3R1^{DA} were treated with NS-siRNA or Orai1-
607 siRNA before measuring Tg-evoked Ca^{2+} entry. Traces show mean ± s.e.m. for 85-
608 100 cells from 3 experiments.

609 (**D**) Summary results (mean ± s.e.m.) show peak increases in $[Ca^{2+}]_c$ ($\Delta[Ca^{2+}]_c$)
610 evoked by Ca^{2+} restoration.

611 (**E**) Tg-evoked Ca^{2+} entry in cells expressing IP_3R1-shRNA with IP_3R1, IP_3R1^{RQ} or
612 $IP_3R1^{RQ/KQ}$. Traces show mean ± s.e.m, for 90-150 cells from 3 experiments.

613 (**F**) Summary results (mean ± s.e.m.) show peak increases in $[Ca^{2+}]_c$ ($\Delta[Ca^{2+}]_c$)
614 evoked by Ca^{2+} restoration. Different letter codes (panels D, F) indicate significantly
615 different values, $P < 0.001$, for multiple comparison one-way ANOVA and pair-wise
616 Tukey's test and for two genotype comparison Mann Whitney U-test.

617 See also **Figure 3 - figure supplement 1.**

618 **Source data in Figure 3 source data file**

619 **Figure 4. Receptor-Regulated IP_3 Production Stimulates SOCE in Cells With**

620 **Empty Ca^{2+} Stores and Expressing Pore-Dead IP_3R**

621 (**A, B**) SH-SY5Y cells expressing IP_3R1-shRNA alone (**A**) or with IP_3R1^{DA} (**B**) were

622 treated with a low concentration of CPA (2 μM) in Ca^{2+}-free HBSS to partially deplete

623 the ER of Ca^{2+} and sub-maximally activate SOCE (see **Figures S5M and S5N**).

624 Carbachol (CCh, 1 μM) was then added to stimulate IP_3 formation through muscarinic

625 receptors, and extracellular Ca^{2+} (2 mM) was then restored. Traces (mean ± s.e.m of

626 68-130 cells from 3 experiments) show responses with and without the CCh addition.

627 (**C**) Summary results show the peak increases in $[Ca^{2+}]_c$ ($\Delta[Ca^{2+}]_c$) after addition of

628 CCh (CCh-induced Ca^{2+} release) and then after restoring extracellular Ca^{2+} (SOCE).

629 (**D-F**) SH-SY5Y cells wild type (WT) (**D**) and expressing NS-shRNA (**E**) or IP_3R1-

630 shRNA (**F**) were treated with YM-254890 (YM, 1 μM, 5 min) in Ca^{2+}-free HBSS to

631 inhibit Gαq and then with thapsigargin (Tg, 1 μM) before restoring extracellular Ca^{2+} (2

632 mM). Traces show mean ± s.e.m of ~120 cells from 3 experiments. .

633 (**G-I**) Similar analyses of HEK cells. Summary results (mean ± s.e.m, 50-100 cells

634 from 3 experiments) are shown in (I).

635 Different letter codes (panels C and I) indicate significantly different values within the

636 store Ca^{2+} release or SOCE groups, $P < 0.001$, one-way ANOVA and pair-wise

637 Tukey's test.

638 See also **Figure 4 - figure supplement 1.**

639 **Source data in Figure 4 source data file**

640

641

642 **Figure 5. IP_3Rs Promote Interaction of STIM1 With Orai1**

643 (**A-E**) PLA analyses of interactions between STIM1 and Orai1 in SH-SY5Y cells

644 expressing NS-shRNA (**A**) or IP_3R1-shRNA alone (**B**) or with IP_3R1 (**C**), IP_3R1^{DA} (**D**)

645 or $IP_3R1^{RQ/KQ}$ (**E**). Confocal images are shown for control cells or after treatment with

646 thapsigargin (Tg, 1 μM) in Ca^{2+}-free HBSS. PLA reaction product is red, and nuclei

647 are stained with DAPI (blue). Scale bars, 5 μm. Summary results show the surface

648 area of the PLA spots for 8-10 cells from 2 independent analyses. Individual values,

649 median (bar) and 25th and 75th percentiles (box). $^{***}P < 0.001$, Student's *t*-test with

650 unequal variances.

651 See also **Figure 5 - figure supplement 1.**

652 **Source data in Figure 5 source data file**

653

654 **Figure 6. Ligand-bound IP_3R1 supports SOCE-dependent STIM1 movement to**
655 **ER-PM contact sites**

656 (**A-B)** Representative TIRF images of mVenus STIM1 co-transfected with either wild
657 type mcherry-rat IP_3R1 (**A**) or $IP_3R1^{RQ/KQ}$ (ligand binding mutant), (**B**) in wild type SH-
658 SY5Y cells before (Basal) and after CPA induced store depletion (CPA treated) at 4
659 min and 7min. On the right are shown RGB profile plots of STIM1 (green) and IP_3R1,
660 wild type or mutant (magenta) corresponding to the rectangular selections (Cell 1 and
661 Cell 2). Scale bar is 10μm.

662 **(C-D)** Changes in number of IP_3R1 (**C**) and STIM1 (**D**) puncta upon CPA-induced
663 store depletion over a period of 10 min in the indicated genotypes. Mean ± s.e.m from
664 7 cells from n=6 independent experiments.

665 **(E)** Summary result (mean ± s.e.m) showing the change in the number of maximum
666 STIM1 puncta formed after CPA-induced store depletion in the indicated genotypes.
667 Mean ± s.e.m. of 7 cells from n=6 independent experiments. Different letters indicate
668 significant differences, $P < 0.05$, Mann-Whitney U-test.

669 See also **Figure 6 - figure supplement 1**.

670 **Source data in Figure 6 source data file.**

671 **Figure 7. Extended Synaptotagmins Rescue SOCE in Cells Lacking IP_3R1**

672 (**A**) SH-SY5Y cells expressing IP_3R1-shRNA alone or with E-Syt1 were stimulated
673 with Tg (1 μM) in Ca^{2+}-free HBSS before restoring extracellular Ca^{2+} (2 mM). Traces
674 show mean ± s.e.m, for 20-80 cells from 3 experiments.

675 (**B**) Summary results show $\Delta[Ca^{2+}]_c$ evoked by restoring Ca^{2+} (SOCE). Mean ± s.e.m,
676 $^{***}P < 0.001$, Mann-Whitney U- test.

677 (**C**) Summary results (mean ± s.e.m, n = 20-80 cells) show resting $[Ca^{2+}]_c$ (left) and
678 the peak Ca^{2+} signals ($\Delta[Ca^{2+}]_c$) evoked by thapsigargin (Tg, 1 μM) in Ca^{2+}-free HBSS
679 for SH-SY5Y cells expressing IP_3R1-shRNA alone or with human E-Syt1.

680 (**D**) Cells over-expressing E-Syt1 and treated with IP_3R1-shRNA in combination with
681 either NS or STIM1 siRNA were stimulated with Tg (1 μM) in Ca^{2+}-free HBSS before
682 restoration of extracellular Ca^{2+} (2 mM). Mean ± s.e.m. from 3 experiments with 30-40
683 cells.

684 (**E, F**) Summary results (mean ± s.e.m, n = 30-40 cells) show SOCE evoked by Tg
685 (**E**), resting $[Ca^{2+}]_c$ and the Tg-evoked Ca^{2+} release from intracellular stores (F). $^{***}P <$
686 0.001, Mann-Whitney U- test.

687 (**G**) Similar analyses of cells expressing NS shRNA alone or with human E-Syt1 and
688 then treated with Tg (1 μM) in Ca^{2+}-free HBSS before restoring extracellular Ca^{2+} (2
689 mM). Mean ± s.e.m. from 3 experiments with 115-135 cells.

690 (**H, I**) Summary results (mean ± s.e.m, n = 115-135 cells) show resting $[Ca^{2+}]_c$ (**H**) and
691 $\Delta[Ca^{2+}]_c$ evoked by Tg (store release) or Ca^{2+} restoration (SOCE) (**I**). No significant
692 difference, Mann Whitney U-test.

693 **Source data in Figure 7 source data file**

694 **Figure 8. Dual Regulation of SOCE by IP_3Rs**

695 (**A**) SOCE is activated when loss of Ca^{2+} from the ER, usually mediated by opening of
696 IP_3Rs when they bind IP_3, causes STIM to unfurl cytosolic domains (2). The exposed
697 cytosolic domains of STIM1 reach across a narrow gap between the ER and PM at a
698 MCS to interact with PIP_2 and Orai1 in the PM. Binding of STIM1 to Orai1 causes pore
699 opening, and SOCE then occurs through the open Orai1 channel. We show that IP_3Rs
700 when they bind IP_3 also facilitate interactions between Orai1 and STIM, perhaps by
701 stabilizing the MCS (1). Receptors that stimulate IP_3 formation thereby promote both
702 activation of STIM (by emptying Ca^{2+} stores) and independently promote interaction of
703 active STIM1 with Orai1.

704 (**B**) Other mechanisms, including ryanodine receptors (RyR), can also release Ca^{2+}
705 from the ER. We suggest that convergent regulation of SOCE by IP_3R with bound IP_3
706 allows receptors that stimulate IP_3 formation to selectively control SOCE.

707 **Figure 1 - figure supplement 1**

708 **Loss of IP_3R1 Attenuates SOCE In Neural Precursor Cells and Differentiated**

709 **Neurons.**

710 (**A-C**) hNPCs expressing NS (**A, C**) or IP_3R1-shRNA (**B**) were stimulated with

711 carbachol (CCh, 100 μM) in Ca^{2+}-free HBSS before restoring extracellular Ca^{2+} (10

712 mM). Each trace shows the Fura 2 fluorescence ratio (F_{340}/F_{380}) from a single cell (>50

713 cells from 3 experiments). Traces in (**C**) show only cells that responded to CCh.

714 (**D, E**) hNPCs expressing shRNA were stimulated with thapsigargin (Tg, 10 μM) in

715 Ca^{2+}-free HBSS before restoring extracellular Ca^{2+} (2 mM). Traces are from individual

716 cells (>180 cells from 3 experiments), with the mean response shown by a thick line.

717 Summary results in **Figures 1D-1G.**

718 (**F**) Confocal images of hNPCs and neurons spontaneously differentiated (10 days)

719 from hNPCs stained for DAPI and neuronal markers: Tuj1 (βIII-tubulin) and NeuN

720 (neuronal nuclear antigen). Scale bars, 50 μm. Only differentiated hNPCs express

721 neuronal markers.

722 (**G**) WB for STIM1 and Orai1 in lysates from hNPCs cells expressing non-silencing

723 (NS) or IP_3R1-shRNA. Summary results (mean ± s.d., n = 3) show relative expression

724 of STIM1 and Orai1 relative to control shRNA (NS) cells. $P > 0.01$, Student's *t*-test

725 with unequal variances.

726 (**H, I**) Spontaneously differentiated hNPCs (25 days) expressing NS (**H**) or IP_3R1-

727 shRNA (**I**) were depolarized by addition of KCl (75 mM). Traces show responses from

728 single cells (>30 cells from 3 experiments) and mean response (thick line).

729 (**J**) Summary results (mean ± s.e.m., 3 experiments) show peak increases in $[Ca^{2+}]_c$

730 ($\Delta[Ca^{2+}]_c$) evoked by depolarization. No significant difference, Student's *t*-test with

731 unequal variances.

732 (**K, L**) Spontaneously differentiated hNPCs expressing NS (**K**) or IP_3R1-shRNA (**L**)

733 were stimulated with Tg (10 μM) in Ca^{2+}-free HBSS before restoring extracellular Ca^{2+}

734 (2 mM). Traces from individual cells (>100 cells from 3 experiments) and the mean

735 response (bold) are shown. Summary results in **Figure 1H-1J.**

736 **Source data in Figure 1 - figure supplement 1 source data file.**

737 **Figure 2 - figure supplement 1**

738 **Reduced Expression of IP_3R1 Using either shRNA or CRISPR/Cas9n Attenuates**

739 **SOCE in SH-SY5Y Cells**

740 (**A, B**) Ca^{2+} signals evoked by carbachol (CCh, 3 μM) in Ca^{2+}-free HBSS in SH-SY5Y

741 cells expressing NS (**A**) or IP_3R1-shRNA (**B**). Traces show responses from single cells

742 (100-200 cells from 3 experiments).

743 (**C, D**) SH-SY5Y cells expressing NS (**C**) or IP_3R1-shRNA (**D**) were treated with

744 thapsigargin (Tg, 1 μM) in Ca^{2+}-free HBSS before restoration of extracellular Ca^{2+} (2

745 mM). Traces show responses from single cells (50-100 cells from 3 experiments) and

746 mean response (thick lines). Summary results in **Figures 2C-2G**.

747 (**E**) Western blots (WB) for STIM1 and Orai1 from lysates of SH-SY5Y cells

748 expressing non-silencing (NS) or IP_3R1-shRNA. Summary results (mean ± s.d., n = 3)

749 show STIM1 and Orai1 expression relative to NS-shRNA cells. $P > 0.05$, Student's *t*-

750 test with unequal variances.

751 (**F**) Western blot for IP_3R1 and tubulin from lysates from WT SH-SY5Y cells and for

752 cells from a cell line in which the IP_3R1 gene was targeted using CRISPR/Cas9 (IKO

753 null). The blot is typical of 3 similar analyses. Summary results (mean ± s.d., n = 3)

754 show IP_3R1 expression relative to WT cells. $P < 0.001$, Student's *t*-test with unequal

755 variances.

756 (**G**) Western blots (WB) for STIM1 (S1), STIM2 (S2) and Orai1 (O1) from lysates of

757 WT and IKO null SH-SY5Y cells. Summary results (mean ± s.d., n = 3) show STIM1,2

758 and Orai1 expression relative to WT cells. $P > 0.05$, Student's t-test with unequal

759 variances.

760 (**H**) Ca^{2+} signals evoked by carbachol (CCh, 1 μM) in WT and IKO null SH-SY5Y cells
761 in Ca^{2+}-free HBSS.
762 (**I**) SH-SY5Y cells (WT or IKO null) were treated with thapsigargin (Tg, 1 μM) in Ca^{2+}-
763 free HBSS before restoring extracellular Ca^{2+} (2 mM). Mean ± s.e.m. from 3
764 experiments with WT cells (black, 110 cells), IKO null cells (red, 117 cells).
765 (**J**) Summary results show the peak increases in $[Ca^{2+}]_c$ evoked by Tg (1 μM) in Ca^{2+}-
766 free HBSS ($\Delta[Ca^{2+}]_c$) and after Ca^{2+} restoration (SOCE). Different letters indicate P <
767 0.001, Mann-Whitney U-test.
768 (**K**) PCRs for IP_3R1 and GAPDH (control gene) of genomic DNA isolated from SH-
769 SY5Y cells. Results (mean ± s.e.m. from 3 independent analyses of a single cell line)
770 are shown for wild type (WT) cells and for cells in which the IP_3R1 gene was targeted
771 using CRISPR/Cas9n (IKO). Expression of IP_3R1 has been normalized to expression
772 of GAPDH. $^{**}P < 0.01$, Student's *t*-test with unequal variances.
773 (**L**) Droplet digital PCR amplification was used to determine gene copy number for
774 IP_3R1 and a control gene RPP30 for WT and IKO SH-SY5Y cells. $^{**}P < 0.05$,
775 Student's *t*-test with unequal variances.
776 **(M)** Western blot for IP_3R1 and tubulin from lysates from WT SH-SY5Y cells and for
777 cells from a cell line in which the IP_3R1 gene was targeted using CRISPR/Cas9n
778 (IKO). The blot is typical of 3 similar analyses. Summary results (mean ± s.d., n = 3)
779 show IP_3R1 expression relative to WT cells. **P < 0.01, Student's *t*-test with unequal
780 variances.
781 (**N**) Ca^{2+} signals evoked by carbachol (CCh, 1 μM) in WT and IKO SH-SY5Y cells in
782 Ca^{2+}-free HBSS. Results show (mean ± s.e.m.) for each of three independently edited

783 cell lines (IKO1, 2 and 3), each with at least 30 cells; and the overall mean ± s.e.m.
784 (red line). Results from a total of 89 WT cells and 130 IKO cells are shown.
785 (**O**) Summary results (mean ± s.e.m. from 3 experiments with 80-100 cells) show peak
786 changes in $[Ca^{2+}]_c$ ($\Delta[Ca^{2+}]_c$) evoked by CCh. ****P* < 0.001, Mann-Whitney U-test.
787 (**P**) SH-SY5Y cells (WT or IKO) were treated with thapsigargin (Tg, 1 μM) in Ca^{2+}-free
788 HBSS before restoring extracellular Ca^{2+} (2 mM). Mean ± s.e.m. from 3 experiments
789 with WT cells (black, 85 cells), 3 independently edited cell lines (IKO 1, 2 and 3; at
790 least 30 cells for each) and the pooled results from all edited cells (97; red).
791 (**Q**) Summary results show the peak increases in $[Ca^{2+}]_c$ evoked by Tg (1 μM) in Ca^{2+}-
792 free HBSS ($\Delta[Ca^{2+}]_c$) and after Ca^{2+} restoration (SOCE). Different letters indicate P <
793 0.001, Mann-Whitney U-test.
794 **Source data in Figure 2 - figure supplement 1 source data file.**

795 **Figure 2 - figure supplement 2**

796 **Attenuated SOCE In SH-SY5Y Cells Lacking IP_3R1 is Rescued by Expression of**

797 **IP_3R1, IP_3R3 or STIM1.**

798 (**A**) Ca^{2+} signals evoked by carbachol (CCh, 3 μM) in SH-SY5Y cells expressing NS or

799 IP_3R1-shRNA, and the latter with IP_3R1 or IP_3R3. Traces show mean ± s.e.m. from >3

800 experiments with 50-70 cells.

801 (**B-D**) Summary results show peak Ca^{2+} signals ($\Delta[Ca^{2+}]_c$) evoked by CCh (**B**), resting

802 $[Ca^{2+}]_c$ (**C**) and the peak Ca^{2+} signal evoked by Tg (10 μM) in Ca^{2+}-free HBSS

803 ($\Delta[Ca^{2+}]_c$, a reporter of ER Ca^{2+} content) (**D**). Different letter codes indicate

804 significantly different values, $P < 0.001$, one-way ANOVA and pair-wise Tukey's test.

805 (**E**) Effects of expressing mCh-STIM1 in SH-SY5Y cells expressing NS shRNA on the

806 Ca^{2+} signals evoked by Tg (1 μM) in Ca^{2+}-free HBSS and then after restoration of

807 extracellular Ca^{2+} (2 mM). Traces show mean ± s.e.m. from 3 experiments with 30-

808 110 cells.

809 (**F**) Summary results show the peak $\Delta[Ca^{2+}]_c$ evoked by restoring extracellular Ca^{2+}

810 after Tg. Mean ± s.e.m. $P > 0.05$, Mann-Whitney U-test.

811 **Source data in Figure 2 - figure supplement 2 source data file.**

812 **Figure 2 - figure supplement 3**

813 **Loss of IP_3R1 Does Not affect SOCE in HEK Cells.**

814 (**A**) WB for IP_3R1 in HEK cells expressing non-silencing (NS) or IP_3R1-shRNA.

815 Summary results (mean ± s.d., n = 3) show IP_3R1 expression relative to tubulin. $^{***}P <$

816 0.001, Student's *t*-test with unequal variances.

817 (**B**) HEK cells expressing NS or IP_3R1-shRNA were treated with thapsigargin (Tg, 1

818 μM) in Ca^{2+}-free HBSS before restoration of extracellular Ca^{2+} (2 mM). Traces show

819 mean response from >100 cells from 3 experiments.

820 (**C**) Summary results show the peak increases in $[Ca^{2+}]_c$ evoked by Tg (1 μM) in Ca^{2+}-

821 free HBSS ($\Delta[Ca^{2+}]_c$, a reporter of ER Ca^{2+} content) and after Ca^{2+} restoration

822 (SOCE).

823 (**D**) Wild type HEK cells (HEK WT) and cells lacking all IP_3Rs (HEK-TKO) were treated

824 with thapsigargin (Tg, 1 μM) in Ca^{2+}-free HBSS before restoration of extracellular Ca^{2+}

825 (2 mM). Traces show mean ± s.e.m. from 3 experiments with 80-120 cells.

826 (**E**) Summary results show the peak $\Delta[Ca^{2+}]_c$ evoked by restoring extracellular Ca^{2+}

827 after Tg. Mean ± s.e.m. $P > 0.01$, Mann-Whitney U-test.

828 (**F**) Proximity ligation assay (PLA) analyses of interactions between STIM1 and Orai1

829 in wild type HEK (WT) and TKO cells. Confocal images are shown for control cells (-

830 Tg) or after10 min treatment with thapsigargin (+Tg, 1 μM) in Ca^{2+}-free HBSS. PLA

831 reaction product is red, and nuclei are stained with DAPI (blue). Scale bars, 5 μm.

832 Summary results show the surface area of the PLA spots for ~20 cells from 2

833 independent analyses. Individual values, median (bar) and 25th and 75th percentiles

834 (box). **P < 0.01, Student's t-test with unequal variances.

835 **Source data in Figure 2 - figure supplement 3 source data file.**

836 **Figure 3 - figure supplement 1**

837 **Attenuated SOCE In SH-SY5Y Cells Lacking IP_3R1 is Rescued by Expression of**

838 **Pore-Dead IP_3R1 with a Functional IP_3-Binding Site.**

839 (**A**) WB with IP_3R1 antibody showing expression of IP_3R1 and IP_3R1^{DA} in SH-SY5Y

840 cells expressing IP_3R1-shRNA.

841 (**B**) Summary (mean ± s.e.m, n = 3) shows IP_3R1 expression normalized to actin. $P <$

842 0.001, one-way ANOVA with pair-wise Tukey's test. Here, and in most subsequent

843 panels, different letters indicate groups that are statistically different, with the test

844 defined for each panel.

845 (**C**) Ca^{2+} signals evoked by carbachol (CCh 3 μM) in SH-SY5Y cells expressing IP_3R1-

846 shRNA alone or with IP_3R1, IP_3R1^{DA}, $IP_3R1^{RQ/KQ}$ or IP_3R1^{1-604}. Traces show mean ±

847 s.e.m. from 3 experiments.

848 (**D**) Summary results (mean ± s.e.m) show peak changes in $[Ca^{2+}]_c$ evoked by CCh

849 ($\Delta[Ca^{2+}]_c$). $P < 0.001$, one-way ANOVA with pair-wise Tukey's test.

850 (**E**) Resting $[Ca^{2+}]_c$ (left) and thapsigargin (Tg)-evoked Ca^{2+} release (1 μM, $\Delta[Ca^{2+}]_c$)

851 (right) in cells treated as indicated. $P < 0.001$, one-way ANOVA with pair-wise Tukey's

852 test.

853 (**F**) WB showing Orai1 expression in cells expressing IP_3R1-shRNA and IP_3R1^{DA}, and

854 then treated with NS or Orai1-siRNA.

855 (**G**) Summary results (normalized to GAPDH expression, mean ± s.d, n =3). $^{**}P <$

856 0.01, Student's t-test with unequal variances.

857 (**H**) Resting $[Ca^{2+}]_c$ (left) and Tg-evoked Ca^{2+} release (right) in cells expressing IP_3R1-
858 shRNA and IP_3R1^{DA}, and then treated with NS or Orai1-siRNA. $P < 0.05$, Mann-
859 Whitney U-test.
860 (**I**) WB for IP_3R1 in cells expressing IP_3R1-shRNA alone or with IP_3R1 or $IP_3R1^{RQ/KQ}$.
861 Results typical of 2 independent experiments.
862 (**J**) Resting $[Ca^{2+}]_c$ (left) and Ca^{2+} release evoked by Tg (right) in cells expressing
863 IP_3R1-shRNA alone or with the indicated IP_3R1. Mean ± s.e.m., $n = 3$ experiments. P
864 < 0.001, one-way ANOVA with pair-wise Tukey's test.
865 (**K**) Changes in $[Ca^{2+}]_c$ evoked by Tg (10 μM) in Ca^{2+}-free HBSS and then after
866 restoration of extracellular Ca^{2+} (2 mM) in cells expressing IP_3R1-shRNA alone or with
867 IP_3R1 or IP_3R1^{1-604}. Mean ± s.e.m. from 3 experiments with >100 cells.
868 **(L**) Summary results show peak increases in $[Ca^{2+}]_c$ evoked by Ca^{2+} restoration in the
869 indicated cells. $P < 0.001$, one-way ANOVA with pair-wise Tukey's test.
870 (**M**) SH-SY5Y cells expressing NS-shRNA were stimulated with the indicated
871 concentrations of CPA in Ca^{2+}-free HBSS to partially deplete ER Ca^{2+} stores and then
872 with ionomycin (Iono, 1 μM) to release all remaining Ca^{2+}. Results show mean ±
873 s.e.m. for >30 cells from 3 experiments.
874 (**N**) Summary results (mean ± s.e.m.) show $\Delta[Ca^{2+}]_c$ evoked by CPA or ionomycin. $P <$
875 0.001, one-way ANOVA with pair-wise Tukey's test. The results confirm that the lower
876 concentrations of CPA partially deplete the ER of Ca^{2+}.
877 **(O**) Summary results (mean ± s.e.m, 80-100 cells from 3 experiments) show the peak
878 increases in $[Ca^{2+}]_c$ ($\Delta[Ca^{2+}]_c$) after adding Tg (store Ca^{2+} release) and after restoring
879 extracellular Ca^{2+} (SOCE) with or without YM-254890 treatment. Different letter codes

880 indicate significantly different values within the Ca^{2+} release or SOCE groups, $P <$

881 0.001, one-way ANOVA and pair-wise Tukey's test.

882 **Source data in Figure 3 - figure supplement 1 source data file.**

883 **Figure 4 - figure supplement 1**

884 **Effects of Generating IP_3 and Inhibiting Gq on Ca^{2+} Signals and STIM1-Orai1**

885 **interactions in SH-SY5Y and HEK Cells.**

886 **(A)** SOCE is enhanced in SH-SY5Y cells expressing control-shRNA after ER-Ca^2

887 depletion (thapsigargin, 2 μM) followed by carbachol (CCh, 1 μM) stimulated IP_3

888 formation. Traces (mean ± s.e.m of ~270 cells each from 5 experiments) show

889 responses with and without the CCh addition. Summary results show the peak

890 increases in $[Ca^{2+}]_c$ ($\Delta[Ca^{2+}]_c$) for SOCE after restoring extracellular Ca^{2+}. Different

891 letters indicate significantly different values of $P < 0.001$ by Mann- Whitney U-test.

892 (**B**) PLA analyses of interactions between STIM1 and Orai1 in wild type (WT) SH-

893 SY5Y cells untreated (-YM) or treated (+YM, 1μm) with Gq inhibitor YM-254890.

894 Confocal images are shown for control cells (-Tg) or after treatment with thapsigargin

895 (+Tg, 1 μM) in Ca^{2+}-free HBSS. PLA reaction product is red, and nuclei are stained

896 with DAPI (blue). Scale bars, 5 μm. Summary results show the surface area of the

897 PLA spots for ~20 cells from 2 independent analyses. Individual values, median (bar)

898 and 25th and 75th percentiles (box). **$P < 0.01$, Student's t-test with unequal

899 variances.

900 (**C**) HEK cells expressing NS shRNA and treated with the Gq inhibitor, YM-254890

901 (YM, 1 μM, 5 min) were stimulated with carbachol (CCh, 100 μM). Traces show mean

902 ± s.e.m. from 3 experiments with 30-40 cells. The results confirm that treatment with

903 YM-254890 effectively uncouples CCh from IP_3-evoked Ca^{2+} signals.

904 (**D**) From results shown in **Figures 4G and 4H**, rates of thapsigargin-evoked Ca^{2+}

905 entry were determined. Summary shows mean ± s.e.m, from 100-120 cells. $P < 0.001$,

906 Mann-Whitney U-test.

907 (**E-F**) Changes in $[Ca^{2+}]_c$ evoked by thapsigargin (Tg, 1 μM) in Ca^{2+}-free HBSS and

908 then after restoration of extracellular Ca^{2+} (2 mM) in WT (**C**) and TKO (**D**) HEK cells

909 after treatment with YM-254890 (YM, 1 μM, 5 min). Traces show mean ± s.e.m. from 3

910 experiments with 100-120 cells.

911 (**G**) Summary results show peak increase in $[Ca^{2+}]_c$ ($\Delta[Ca^{2+}]_c$) evoked by addition of

912 thapsigargin and then after restoring extracellular Ca^{2+} (SOCE). Mean ± s.e.m.

913 Different letter codes indicate significantly different values, $P < 0.001$, Mann- Whitney

914 U-test.

915 **Source data in Figure 4 - figure supplement 1 source data file.**

916 **Figure 5 - figure supplement 1**

917 **Validation of PLA Measurements of Orai1-STIM1 Interactions.**

918 (**A**) PLA using antibodies to Orai1 and STIM1 to establish whether they are
919 associated. Complementary oligonucleotides conjugated to a secondary antibody (2nd)
920 targeting their respective primary antibodies (1st) hybridize when they are close to
921 each other, allowing rolling circle amplification (RCA) and production of a red
922 fluorescent product. The latter can be quantified from the surface area of the
923 fluorescent spots or their intensity. We obtained indistinguishable results with both
924 methods of quantification. We therefore show only results obtained from surface-area
925 measurements.

926 (**B-D**) Confocal images from PLA assays of SH-SY5Y cells expressing NS-shRNA
927 performed with no primary antibody (**B**), or with primary antibody for only STIM1 (**C**) or
928 only Orai1 (**D**). Scale bars, 5 µm.

929 (**E, F**) Confocal images of SH-SY5Y cells expressing NS-shRNA with (**F**) or without
930 thapsigargin treatment (**E**) (Tg, 1 µM, in Ca^{2+}-free HBSS). Cells are stained with DAPI
931 and immunostained for Orai1 or STIM1. Scale bars, 5 µm.

932 **(G-N)** Similar analyses of cells expressing IP_3R1-shRNA alone (**G, H**), or with IP_3R1 (**I,**
933 **J**), IP_3R1^{DA} (**K, L**) or $IP_3R1^{RQ/KQ}$ (**M, N**). Results (**E-N**) are typical of 2 experiments.

934 **(O)** Number of PLA spots per cell in the indicated genotypes with (5 min) or without (0
935 min) thapsigargin treatment (Tg, 1 µM in Ca^{2+}-free HBSS) in the indicated genotypes.
936 Different letter indicates significantly different values, $P < 0.001$ one-way ANOVA and
937 pair-wise Tukey's test.

938 The PLA results are shown in **Figure 5**.

939 **Figure 6 - figure supplement 1**

940 **Validation of fluorescent-tagged rat IP_3R1 constructs**

941 **(A)** Western blot image showing the expression of IP_3R1 in the indicated genotypes

942 Results with these constructs are shown in **Figure 6.**

943 **Source data in Figure 6 – figure supplement 1.**

944 **RESOURCE AVAILABILITY**

945 **Lead Contact**

946 All requests for resources and reagents should be directed to the lead contact, Dr.
947 Gaiti Hasan (gaiti@ncbs.res.in).

948

949 **Materials Availability**

950 Constructs and cell lines are available upon request. MTA required for cell lines.

951

952 **Data and Code Availability**

953 This study did not generate any computer code. The data supporting the findings of
954 this study are available within the manuscript. All other data supporting the findings of
955 this study are available in source data file of respective figures.

956

957 **METHOD DETAILS**

958 **Culture of Human Neural Precursor Cells**

959 Human neural precursor cells (hNPCS) were derived from a human embryonic stem
960 cell (hESC) line, H9/WA09 (RRID: CVCL_9773), using a protocol that inhibits dual
961 SMAD signalling and stimulates Wnt signaling (Reinhardt *et al.*, 2013) as described
962 previously (Gopurappilly *et al.*, 2018, 2019). hNPCs were grown as adherent
963 dispersed cells on growth factor-reduced Matrigel (0.5%, Corning, Cat#356230) in
964 hNPC maintenance medium (NMM) at 37°C in humidified air with 5% CO_2. NMM
965 comprised a 1:1 mixture of Dulbecco's Modified Eagle Medium with Nutrient Mixture
966 F-12 (DMEM/F-12, Invitrogen, Cat#10565018) and Neurobasal medium

967 (ThermoFisher, Cat#21103049), supplemented with GlutaMAX (0.5x, ThermoFisher,
968 Cat#35050061), N2 (1:200, ThermoFisher, 17502048), B27 without vitamin A (1:100,
969 ThermoFisher, Cat#12587010), Antibiotic-Antimycotic (ThermoFisher,
970 Cat#15240112), CHIR99021 (3 μM, STEMCELL Technologies, Cat#72052),
971 purmorphamine (0.5 mM, STEMCELL Technologies, Cat#72202) and ascorbic acid
972 (150 μM, Sigma, Cat#A92902). Doubling time was ~24 hr. Cells were passaged every
973 4-5 days by treatment with StemPro Accutase (ThermoFisher, Cat#A1110501), stored
974 in liquid nitrogen, and thawed as required. Cells were confirmed to be mycoplasma-
975 free by monthly screening (MycoAlert, Lonza, Cat#LT07-318). hNPCs between
976 passages 16-19 were used.
977 All experiments performed with hESC lines were approved by the Institutional
978 Committee for Stem Cell Research, registered under the National Apex Committee for
979 Stem Cell Research and Therapy, Indian Council of Medical Research, Ministry of
980 Health, New Delhi.

981 **Stable Knockdown of IP_3R1**

982 An UltramiR lentiviral inducible shRNA-mir based on the shERWOOD algorithm
983 (Auyeung *et al.*, 2013; Knott *et al.*, 2014) was used to inhibit IP_3R1 expression. The
984 all-in-one pZIP vector, which allows puromycin-selection and doxycycline-induced
985 expression of both shRNA-mir and Zs-Green for visualization, was from TransOMIC
986 Technologies (Huntsville, AL). Lentiviral pZIP transfer vectors encoding non-silencing
987 shRNA (NS, NT#3-TTGGATGGGAAGTTCACCCCG) or IP_3R1-targeting shRNA
988 (ULTRA3316782- TTTCTTGATCACTTCCACCAG) were packaged as lentiviral
989 particles using packaging (pCMV- dR8.2 dpvr, Addgene, plasmid #8455) and

990 envelope vectors (pCMV-VSV-G, Addgene, plasmid #8454) by transfection of
991 HEK293T cells (referred as HEK, ATCC, Cat# CRL-3216). Viral particles were
992 collected and processed and hNPCs (passage 9) or SH-SY5Y cells were transduced
993 (multiplicity of infection, MOI = 10) using Lipofectamine LTX with PLUS reagent
994 (ThermoFisher, Cat#15338100). Cells were maintained in media containing
995 doxycycline (2 µg/ml, Sigma, Cat# D3072) to induce shRNA expression, and
996 puromycin to select transduced cells (1 µg/ml for hNPCs; 3 µg/ml for SH-SY5Y cells;
997 Sigma, Cat# P9620). Cells were passaged 4-5 times after lentiviral transduction to
998 select for stable expression of shRNAs.

999 **Derivation of Neurons From hNPCs**

1000 Neurons were differentiated from hNPCs stably transduced with shRNA. hNPCs were
1001 seeded at 50-60% confluence in NMM on coverslips coated with poly-d-lysine (0.2
1002 mg/ml, Sigma, Cat#P7280). After 1-2 days, the medium was replaced with neuronal
1003 differentiation medium, which comprised a 1:1 mixture of DMEM/F-12 with Neurobasal
1004 supplemented with B27 (1:100), N2 (1:200), GlutaMAX (0.5x) and Antibiotic-
1005 Antimycotic solution. Medium was replaced on alternate days. Neurons were used
1006 after 15-20 days.

1007 **Culture and Transfection of SH-SY5Y Cells**

1008 SH-SY5Y cells (ATCC, USA, Cat# CRL-2266) were grown on culture dishes in
1009 DMEM/F-12 with 10% fetal bovine serum (Sigma, Cat# F4135) at 37 °C in humidified
1010 air with 5% CO_2. Cells were passaged every 3-4 days using TrypLE Express
1011 (ThermoFisher, Cat# 12605036) and confirmed to be free of mycoplasma. Cells
1012 expressing shRNA were transiently transfected using TransIT-LT1 reagent (Mirus,

1013 Cat# MIR-2300) in Opti-MEM (ThermoFisher, Cat# 31985062). Plasmids (250 ng)
1014 and/or siRNA (200 ng) in transfection reagent (1 µg/2.5 µl) were added to cells grown
1015 to 50% confluence on glass coverslips attached to an imaging dish. Cells were used
1016 after 48 hrs. The siRNAs used were to human Orai1 (100 nM, Dharmacon, Cat# L-
1017 014998-00-0005) or non-silencing (NS, Dharmacon, Cat# D-495 001810-10-05), to
1018 human STIM1 (Santa Cruz Biotechnology, Cat# sc-76589) or NS (Santa Cruz
1019 Biotechnology, Cat# sc-37007). The expression plasmids were IP_3R1 (rat type 1
1020 IP_3R1 in pcDNA3.2/V5DEST vector) (Dellis *et al.*, 2008), rat IP_3R1^{DA} (D2550 replaced
1021 by A in pcDNA3.2 vector) (Dellis *et al.*, 2008), rat IP_3R1^{RQ} (R568 replaced by Q of type
1022 1 IP_3R in pCDNA3.2/V5DEST vector) (Dellis *et al.*, 2008), rat $IP_3R1^{RQ/KQ}$ (R568 and
1023 K569 replaced by Q of type 1 IP_3R in pCDNA3.2/V5DEST vector), rat IP_3R1^{1-604}
1024 (residues 1-604 of IP_3R with N-terminal GST tag in pCDNA3.2/V5DEST vector) (Dellis
1025 *et al.*, 2008), rat IP_3R3 (rat type 3 IP_3R in pcDNA3.2/V5DEST vector) (Saleem *et al.*,
1026 2013), human mCherry-STIM1 (N terminal mCherry tagged human STIM1 in
1027 pENTR1a vector) (Nunes-Hasler *et al.*, 2017) and human extended synaptotagmin 1
1028 (E-Syt1), a kind gift from Dr S. Muallem, NIDCR, USA (Maléth *et al.*, 2014).

1029 **CRISPR/Cas9 and Cas9n Editing of SH-SY5Y Cells**

1030 To allow either CRISPR/Cas9 or Cas9n-mediated disruption of IP_3R1 expression, we
1031 used a published method to clone gRNAs into the backbone vector (pSpCas9n(BB)-
1032 2A-Puro PX462 V2.0, Addgene, Cat#62987) (Ran *et al.*, 2013). Forward and reverse
1033 sgRNA oligonucleotides (100 µM) were annealed and ligated using T4 DNA ligase by
1034 incubation (10 µl, 37°C, 30 min) before slow cooling to 20°C. Plasmids encoding
1035 Cas9n were digested with *BbsI-HF* (37°C, 12 hr), gel-purified (NucleoSpin Gel and

1036 PCR Clean-up kit from Takara) and the purified fragment was stored at -20°C. A
1037 mixture (final volume 20 µl) of gRNA duplex (1 µl, 0.5 µM), digested px459 (for IKO
1038 null) or pX462 vector (for IKO) (30 ng), 10× T4 DNA ligase buffer (2 µl) and T4 DNA
1039 ligase (1 µl) was incubated (20°C, 1 hr). After transformation of DH5-α competent *E.*
1040 *coli* with the ligation mixture, plasmids encoding Cas9 or Cas9n and the sgRNAs were
1041 extracted, and the coding sequences were confirmed (Ran *et al.*, 2013). The plasmid
1042 (2 µg) was then transfected into SH-SY5Y cells (50-60% confluent) in a 6-well plate
1043 using TransIT LT-1 reagent (Mirus Bio, Cat# MIR-2300). After 48 hr, puromycin (3
1044 µg/ml, 72 hr) was added to kill non-transfected cells. IKO colonies were propagated
1045 and screened for Ca^{2+} signals evoked by carbachol and for the presence of the IP_3R
1046 gene by genomic DNA PCR and droplet digital PCR using primers close to the region
1047 targeted by the gRNAs (Miotke *et al.*, 2014). Three independently derived IKO lines,
1048 each with one residual IP_3R1 gene, were used for analyses of Ca^{2+} signaling (see
1049 **Figure S2N-S2Q**). For one of the cell lines (IKO 2), disruption of one copy of the
1050 IP_3R1 gene was confirmed by genomic PCR, droplet digital PCR and Western blotting
1051 (**Figures S2K-S2M**). For the IKO null line, single cell selection was done in a 96 well
1052 plate setup followed by screening for carbachol-evoked Ca^{2+} signals from multiple
1053 clones. A single clone was selected (**Figure S2H**) and a western blot performed to
1054 confirm absence of IP_3R1 expression (**Figure S2F**). All the oligonucleotide
1055 sequences are described in **supplementary file 1.**
1056
1057
1058

1059 **Plasmid construction**

1060 Mutagenesis and all DNA modifications were carried out using *Q5* Hot Start high-
1061 fidelity 2X Master Mix (New England BioLabs, Cat# M0494L) using the
1062 recommendations of the manufacturer. Primers used in this study (details given in
1063 **supplementary file 1**) were synthesized by Integrated DNA Technologies (IDT).
1064 Mutations in the Ligand binding domain (R568Q and K569Q) of IP_3R1 were generated
1065 on the rat mCherry-IP_3R1 cDNA in pDNA3.1 Mutations in all the constructs were
1066 confirmed by sequencing.

1067 **Ca^{2+} Imaging**

1068 Methods for single-cell Ca^{2+} imaging were described previously (Gopurappilly *et al.*,
1069 2019)**.** Briefly, cells grown as a monolayer (~70% confluence) on homemade
1070 coverslip-bottomed dishes were washed and loaded with Fura 2 by incubation with
1071 Fura 2 AM (4 μM, 45 min, 37°C, ThermoFisher, Cat# F1221), washed and imaged at
1072 room temperature in HEPES-buffered saline solution (HBSS). HBSS comprised: 20
1073 mM HEPES, 137 mM NaCl, 5 mM KCl, 2 mM $MgCl_2$, 2 mM $CaCl_2$, 10 mM glucose, pH
1074 7.3. $CaCl_2$ was omitted from Ca^{2+}-free HBSS. Treatments with carbachol (CCh,
1075 Sigma, Cat# C4382), thapsigargin (Tg, ThermoFisher, Cat# 7458), cyclopiazonic acid
1076 (CPA, Sigma Cat# C1530) or high-K^+ HBSS (HBSS supplemented with 75 mM KCl)
1077 are described in legends.

1078 Responses were recorded at 2-s intervals using an Olympus IX81-ZDC2 Focus
1079 Drift-Compensating Inverted Microscope with 60× oil immersion objective (numerical
1080 aperture, NA = 1.35) with excitation at 340 nm and 380 nm. Emitted light (505 nm)
1081 was collected with an Andor iXON 897E EMCCD camera and AndoriQ 2.4.2 imaging

1082 software (RRID: SCR_014461). Maximal (R_{max}) and minimal (R_{min}) fluorescence ratios
1083 were determined by addition of ionomycin (10 μM, Sigma, Cat# 407953) in HBSS
1084 containing 10 mM $CaCl_2$ or by addition of Ca^{2+}-free HBSS containing BAPTA (10 mM,
1085 Sigma, Cat# 196418) and Triton X100 (0.1%). Background-corrected fluorescence
1086 recorded from regions of interest ROI) drawn to include an entire cell was used to
1087 determine mean fluorescence ratios ($R = F_{340}/F_{380}$) (ImageJ), and calibrated to $[Ca^{2+}]_c$
1088 from (Grynkiewicz, Poenie and Tsien, 1985):

1089 $$[Ca^{2+}]_c = K_D \cdot {F_{380}^{min}}/{F_{380}^{max}} \cdot {(R - R_{min})}/{(R_{max} - R)}$$

1090 where, K_D = 225 nM (Forostyak *et al.*, 2013).

1091

1092 **Western Blots**

1093 Proteins were isolated in RIPA buffer (Sigma, Cat# R0278) with protease inhibitor
1094 cocktail (Sigma, Cat# P8340) or, for WB of Orai1, in medium containing 150 mM
1095 NaCl, 50 mM Tris, 1% Triton-X-100, 0.1% SDS and protease inhibitor cocktail. After
1096 30 min on ice with intermittent shaking, samples were collected by centrifugation
1097 (11,000 ×*g*, 20 min) and their protein content was determined (Thermo Pierce BCA
1098 Protein Assay kit, ThermoFisher, Cat# 23225). Proteins (~30 μg/lane) were separated
1099 on 8% SDS-PAGE gels for IP_3R or 10% SDS-PAGE gels for STIM1 and Orai1, and
1100 transferred to a Protran 0.45-μm nitrocellulose membrane (Merck, Cat# GE10600003)
1101 using a TransBlot semi-dry transfer system (BioRad, Cat# 1703940). Membranes
1102 were blocked by incubation (1 hr, 20°C) in TBST containing skimmed milk or bovine
1103 serum albumin (5%, Sigma, Cat# A9418). TBST (Tris-buffered saline with Tween)

1104 comprised: 137 mM NaCl, 20 mM Tris, 0.1% Tween-20, pH 7.5. Membranes were
1105 incubated with primary antibody in TBST (16 hr, 4°C), washed with TBST (3 ×10 min),
1106 incubated (1 hr, 20°C) in TBST containing HRP-conjugated secondary antibody
1107 (1:3000 anti-mouse, Cell Signaling Technology Cat# 7076S; or 1:5000 anti-rabbit,
1108 ThermoScientific Cat# 32260). After 3 washes, HRP was detected using Pierce ECL
1109 Western Blotting Substrate (ThermoFisher, Cat# 32106) and quantified using
1110 ImageQuant LAS 4000 (GE Healthcare) and Image J. The primary antibodies used
1111 were to: IP_3R1 (1:1000, ThermoFisher, Cat# PA1-901, RRID: AB_2129984); β-actin
1112 (1:5000, BD Biosciences, Cat# 612656, RRID: AB_2289199); STIM1 (1:1000, Cell
1113 Signaling Technology, Cat# 5668S, RRID: AB_10828699); Orai1 (1:500, ProSci, Cat#
1114 PM-5205, RRID: AB_10941192); IP_3R2 (1:1000, custom made by Pocono Rabbit
1115 Farm and Laboratory) (Mataragka and Taylor, 2018); and IP_3R3 (1:500, BD
1116 Biosciences, Cat# 610313, RRID: AB_397705).

1117 **Immunocytochemistry**

1118 After appropriate treatments, cells on a coverslip-bottomed plate were washed twice
1119 with cold PBS, fixed in PBS with paraformaldehyde (4%, 20°C, 20 min), washed (3 × 5
1120 min) with PBS containing Triton-X100 (0.1%, PBST) and blocked by incubation (1 hr,
1121 20°C) in PBST containing goat serum (5%). After incubation with primary antibody in
1122 PBST (16 hr, 4°C) and washing with PBST (3 × 5 min), cells were incubated (1 hr,
1123 20°C) with secondary antibody in PBST containing goat serum, washed (3 × 5 min),
1124 stained (10 min, 20°C) with DAPI (1 μg/ml in PBS; Sigma, Cat# D9542) and washed
1125 (5 min, PBST). Cells were then covered with glycerol (60% v/v) and imaged using an
1126 Olympus FV300 confocal laser scanning microscope with 20× or 60× oil-immersion

1127 objectives. Fluorescence was analyzed using ImageJ. The primary antibodies used
1128 were to: PAX6 (1:500, Abcam, Cat# ab195045, RRID: AB_2750924); Nestin (1:500,
1129 Abcam, Cat# 92391, RRID: AB_10561437); Ki67 (1:250, Abcam, Cat# ab16667,
1130 RRID: AB_302459); SOX1 (1:1000, Abcam, Cat# ab87775, RRID: AB_2616563); Tuj1
1131 (βIII Tubulin 1:1000, Promega, Cat# G712, RRID: AB_430874); NeuN (1:300, Abcam,
1132 Cat# ab177487, RRID: AB_2532109); Doublecortin (1:500, Abcam, Cat# 18723,
1133 RRID: AB_732011); MAP2 (1:200, Abcam, Cat# ab32454, RRID: AB_776174); STIM1
1134 (1:1000, Cell Signaling Technology, Cat# 5668S, RRID: AB_10828699); and Orai1
1135 (1:500, ProSci, Cat# PM-5205, RRID: AB_10941192).

1136 **Proximity Ligation Assay**

1137 The Duolink *In Situ* Red Starter Mouse/Rabbit kit was from Sigma (#Cat DUO92101)
1138 and used according to the manufacturer's protocol with primary antibodies to Orai1
1139 (mouse 1:500) and STIM1 (rabbit 1:1000). Cells (~30% confluent) were treated with
1140 thapsigargin (1 μM, 5 min) in Ca^{2+}-free HBSS before fixation, permeabilization, and
1141 incubation with primary antibodies (16 hr, 4°C) and the PLA reactants. Red
1142 fluorescent PLA signals were imaged using an Olympus FV300 confocal laser
1143 scanning microscope, with excitation at 561 nm, and a 60× oil-immersion objective.
1144 Quantitative analysis of the intensity and surface area of PLA spots used the "Analyze
1145 particle" plugin of Fiji. Results are shown for 8-10 cells from two biological replicates of
1146 each genotype.

1147 **Detection of STIM1 and IP_3R1 puncta using TIRF microscopy**

1148 SHSY5Y cells were cultured on 15 mm glass coverslips coated with poly-D-lysine
1149 (100 μg/ml) in a 35 mm dish for 24 h. Cells were co-transfected with 500 ng of

1150 mCherry rIP_3R1 and 200 ng mVenus STIM1 plasmids using TransIT-LT1 transfection
1151 reagent in Opti-MEM. Following 48 h of transfection and prior to imaging, cells were
1152 washed with imaging buffer (10 mM HEPES, 1.26 mM Ca^{2+}, 137 mM NaCl, 4.7 mM
1153 KCl, 5.5 mM glucose, 1 mM Na_2HPO_4, 0.56 mM $MgCl_2$, at pH 7.4). The coverslips
1154 were mounted in a chamber and imaged using an Olympus IX81 inverted total internal
1155 reflection fluorescence microscope (TIRFM) equipped with oil-immersion PLAPO
1156 OTIRFM 60× objective lens/1.45 numerical aperture and Hamamatsu ORCA-Fusion
1157 CMOS camera. Olympus CellSens Dimensions 2.3 (Build 189987) software was used
1158 for imaging. The angle of the excitation beam was adjusted to achieve TIRF with a
1159 penetration depth of ∼130 nm. Images were captured from a final field of 65 μm × 65
1160 μm (300 × 300 pixels, one pixel=216 nm, binning 2×2). Cells positive for both mCherry
1161 rIP_3R1 and mVenus STIM1 were identified using 561 nm and 488 nm lasers,
1162 respectively. The cells were incubated in zero calcium buffer (10 mM HEPES, 1 mM
1163 EGTA, 137 mM NaCl, 4.7 mM KCl, 5.5 mM glucose, 1 mM Na2HPO4, 0.56 mM
1164 MgCl2, at pH 7.4) for 2 minutes followed by addition of 30 μM CPA in zero calcium
1165 buffer. IP_3R1 and STIM1 puncta prior to CPA addition and after CPA addition were
1166 captured at 1 min intervals. Raw images were filtered for background correction and
1167 same setting was used across all samples. Regions where fresh STIM1 puncta (0.2-
1168 10 pixels) appeared post-CPA treatment at 10 mins were marked and subsequently
1169 IP_3R1 puncta (0.2-10 pixels) were captured from the same region. Particle analysis
1170 and RGB profile plot were done using ImageJ.
1171
1172

1173 **Statistical Analyses**

1174 All experiments were performed without blinding or prior power analyses. Independent
1175 biological replicates are reported as the number of experiments (n), with the number
1176 of cells contributing to each experiment indicated in legends. The limited availability of
1177 materials for PLA restricted the number of independent replicates (n) to 2 (each with
1178 8-10 cells). Most plots show means ± s.e.m. (or s.d.). Box plots show 25th and 75th
1179 percentiles, median and mean (see legends). Where parametric analyses were
1180 justified by a Normality test, we used Student's *t*-test with unequal variances for 2-way
1181 comparisons and ANOVA followed by pair-wise Tukey's test for multiple comparisons.
1182 Non-parametric analyses used the Mann-Whitney U-test. Statistical significance is
1183 shown by $^{***}P < 0.001$, $^{**}P < 0.01$, $^{*}P < 0.05$, or by letter codes wherein different letters
1184 indicate significantly different values ($P < 0.001$, details in legends). All analyses used
1185 Origin 8.5 software.

1186

1187 **Details of the plasmids and recombinant DNAs are given in Supplementary file**
1188 **1.**

1189

1190 **Source data files**

1191 Figure 1 source data

1192 Figure 2 source data

1193 Figure 3 source data

1194 Figure 4 source data

1195 Figure 5 source data

1196 Figure 6 source data

1197 Figure 7 source data

1198 Figure 1 – figure supplement 1 source data

1199 Figure 2 – figure supplement 1 source data

1200 Figure 2 – figure supplement 2 source data

1201 Figure 2 – figure supplement 3 source data

1202 Figure 3 – figure supplement 1 source data

1203 Figure 4 – figure supplement 1 source data

1204 Figure 6 – figure supplement 1 source data

Figure 1

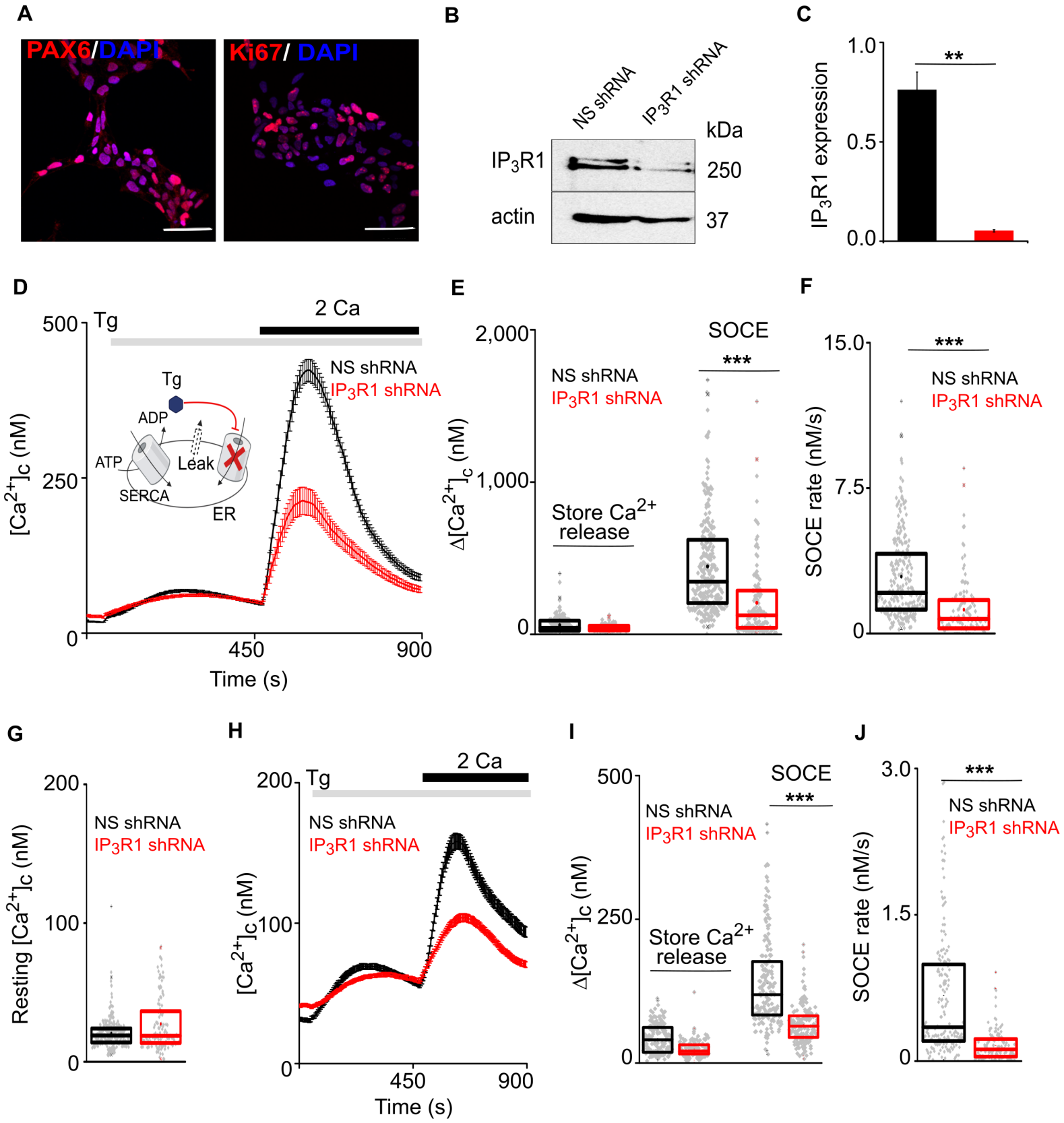
A
PAX6/DAPI
Ki67/ DAPI
B
NS shRNA
IP3R1 shRNA
kDa
IP3R1
250
actin
37
C
IP3R1 expression
1.0
0.5
0.0
**
D
Tg
2 Ca
500
250
0
[Ca2+]c (nM)
NS shRNA
IP3R1 shRNA
Tg
ADP
ATP
Leak
SERCA
ER
450
900
Time (s)
E
SOCE
2,000
1,000
0
Δ[Ca2+]c (nM)
NS shRNA
IP3R1 shRNA
***
Store Ca2+ release
F
15.0
7.5
0
SOCE rate (nM/s)
***
NS shRNA
IP3R1 shRNA
G
200
100
0
Resting [Ca2+]c (nM)
NS shRNA
IP3R1 shRNA
H
Tg
2 Ca
200
100
0
[Ca2+]c (nM)
NS shRNA
IP3R1 shRNA
450
900
Time (s)
I
SOCE
500
250
0
Δ[Ca2+]c (nM)
NS shRNA
IP3R1 shRNA
***
Store Ca2+ release
J
3.0
1.5
0
SOCE rate (nM/s)
***
NS shRNA
IP3R1 shRNA

Figure 2

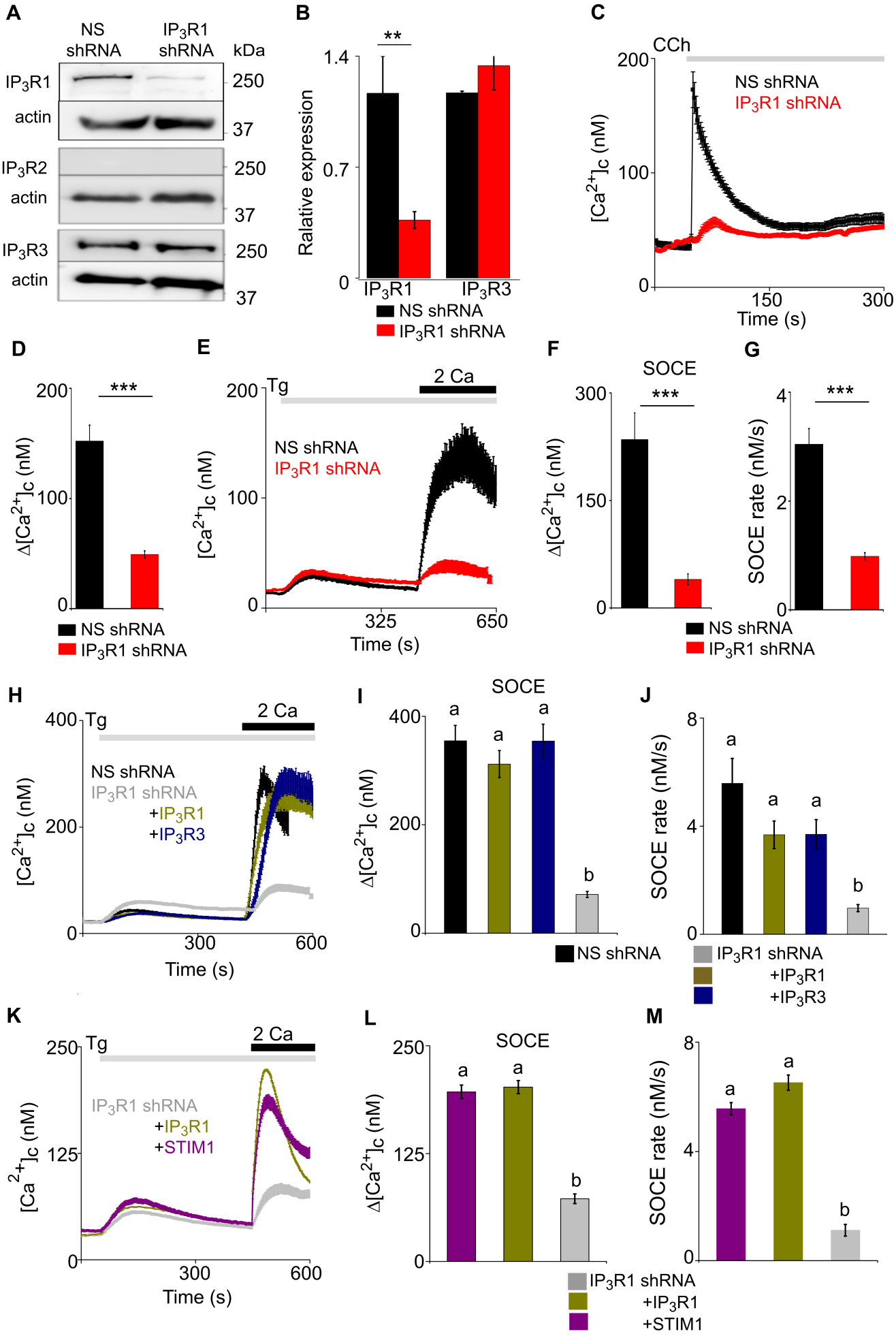
A
NS shRNA
IP3R1 shRNA
kDa
IP3R1
actin
IP3R2
IP3R3
250
37
B
**
Ralative expression
1.4
0.7
0
IP3R1
IP3R3
NS shRNA
IP3R1 shRNA
C
CCh
200
100
0
NS shRNA
IP3R1 shRNA
[Ca2+]c (nM)
150
300
Time (s)
D
***
Δ[Ca2+]c (nM)
NS shRNA
IP3R1 shRNA
E
Tg
2 Ca
NS shRNA
IP3R1 shRNA
[Ca2+]c (nM)
325
650
Time (s)
F
SOCE
***
Δ[Ca2+]c (nM)
G
SOCE rate (nM/s)
H
Tg
2 Ca
NS shRNA
IP3R1 shRNA
+IP3R1
+IP3R3
[Ca2+]c (nM)
300
600
Time (s)
I
SOCE
a
b
Δ[Ca2+]c (nM)
NS shRNA
J
SOCE rate (nM/s)
IP3R1 shRNA
+IP3R1
+IP3R3
K
Tg
2 Ca
IP3R1 shRNA
+IP3R1
+STIM1
[Ca2+]c (nM)
125
Time (s)
L
SOCE
Δ[Ca2+]c (nM)
M
SOCE rate (nM/s)
IP3R1 shRNA
+IP3R1
+STIM1

Figure 3

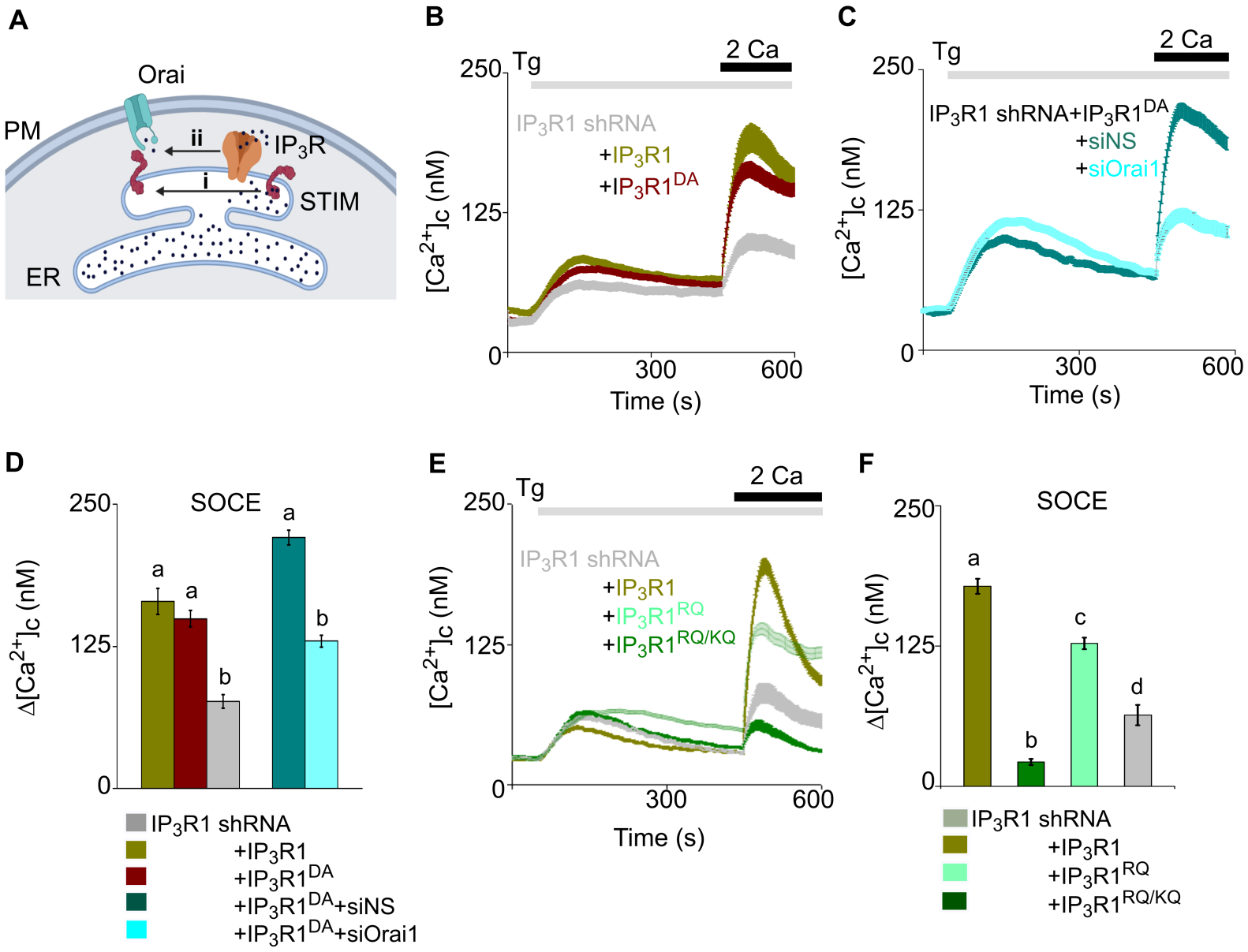
A
Orai
PM
ii
IP3R
i
STIM
ER
B
Tg
2 Ca
250
125
0
IP3R1 shRNA
+IP3R1
+IP3R1DA
[Ca2+]c (nM)
300
600
Time (s)
C
Tg
2 Ca
IP3R1 shRNA+IP3R1DA
+siNS
+siOrai1
D
SOCE
Δ[Ca2+]c (nM)
a
a
b
a
b
IP3R1 shRNA
+IP3R1
+IP3R1DA
+IP3R1DA+siNS
+IP3R1DA+siOrai1
E
Tg
2 Ca
IP3R1 shRNA
+IP3R1
+IP3R1RQ
+IP3R1RQ/KQ
F
SOCE
a
b
c
d
IP3R1 shRNA
+IP3R1
+IP3R1RQ
+IP3R1RQ/KQ

Figure 4

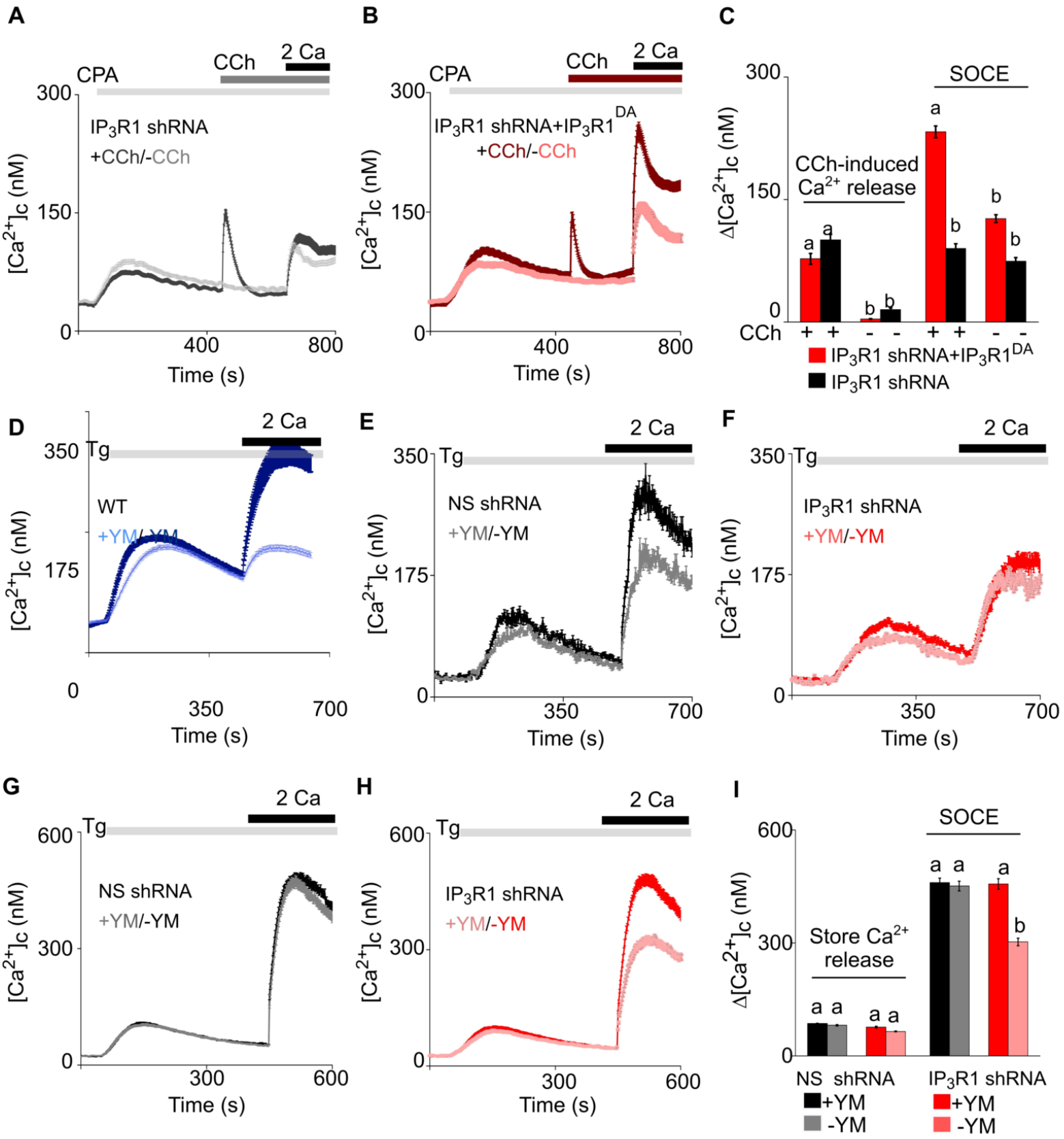
A
CPA
CCh
2 Ca
IP3R1 shRNA
+CCh/-CCh
[Ca2+]c (nM)
Time (s)
B
CPA
CCh
2 Ca
IP3R1 shRNA+IP3R1DA
+CCh/-CCh
C
SOCE
CCh-induced Ca2+ release
Δ[Ca2+]c (nM)
CCh
IP3R1 shRNA+IP3R1DA
IP3R1 shRNA
D
Tg
2 Ca
WT
+YM/-YM
E
NS shRNA
+YM/-YM
F
IP3R1 shRNA
+YM/-YM
G
NS shRNA
+YM/-YM
H
IP3R1 shRNA
+YM/-YM
I
SOCE
Store Ca2+ release
NS shRNA
IP3R1 shRNA
+YM
-YM

Figure 5

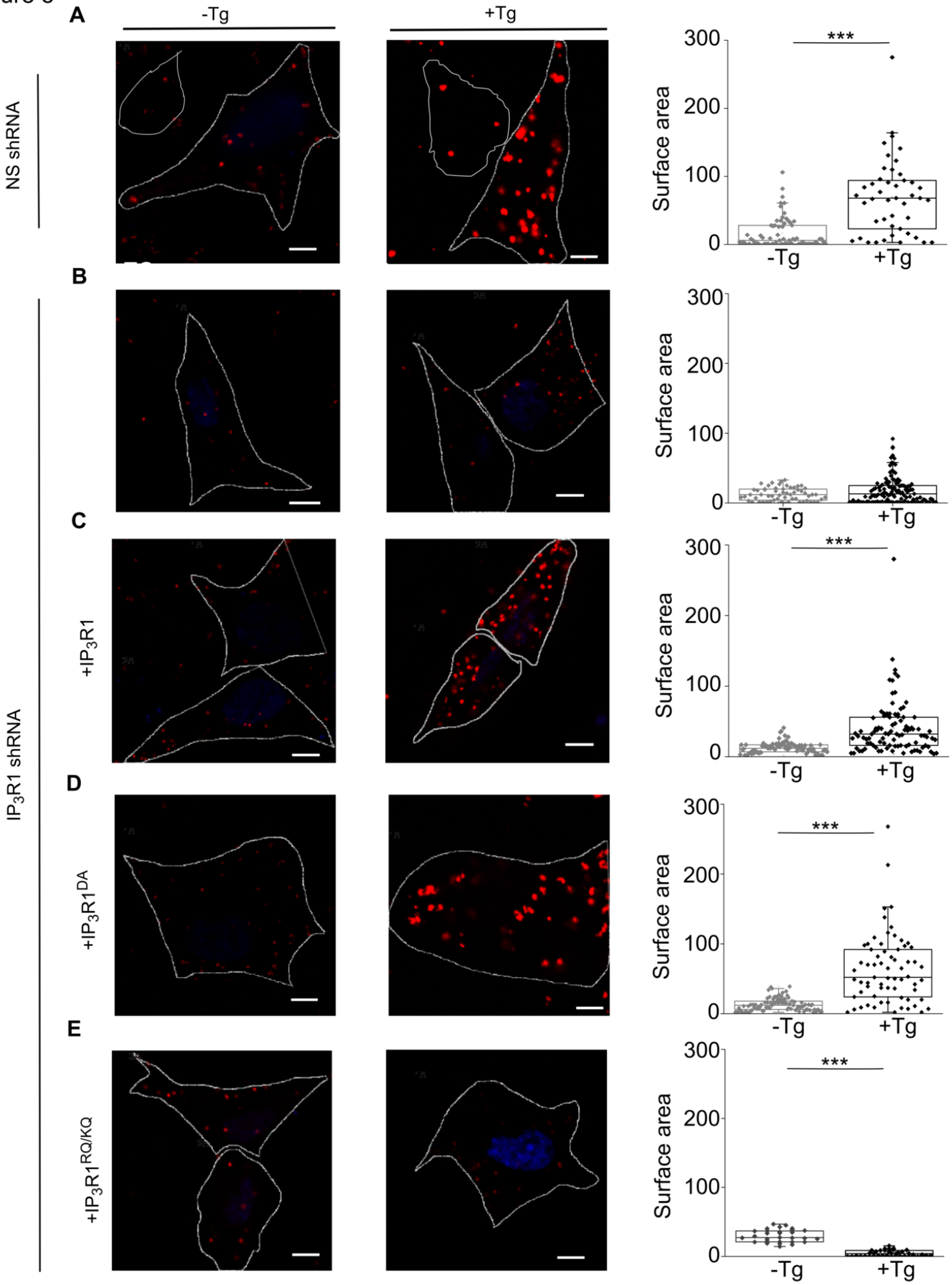
A
-Tg
+Tg
NS shRNA
B
C
+IP3R1
D
+IP3R1DA
E
+IP3R1RQ/KQ
IP3R1 shRNA
Surface area
300
200
100
0
-Tg
+Tg
***

Figure 6

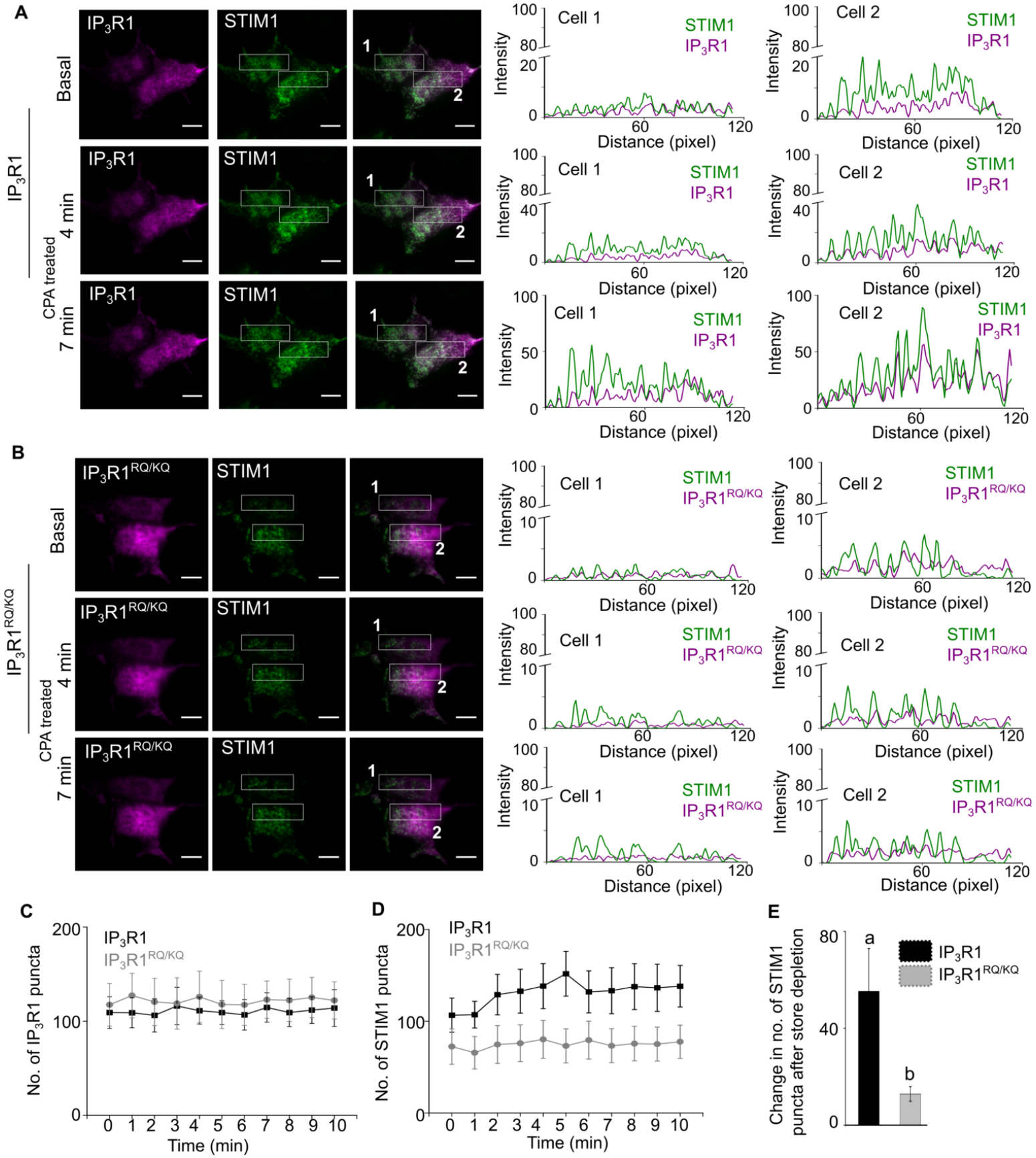
A
IP3R1
STIM1
Basal
4 min
7 min
CPA treated
Cell 1
Cell 2
Intensity
Distance (pixel)
B
IP3R1RQ/KQ
C
No. of IP3R1 puncta
Time (min)
D
No. of STIM1 puncta
E
Change in no. of STIM1 puncta after store depletion
a
b

Figure 7

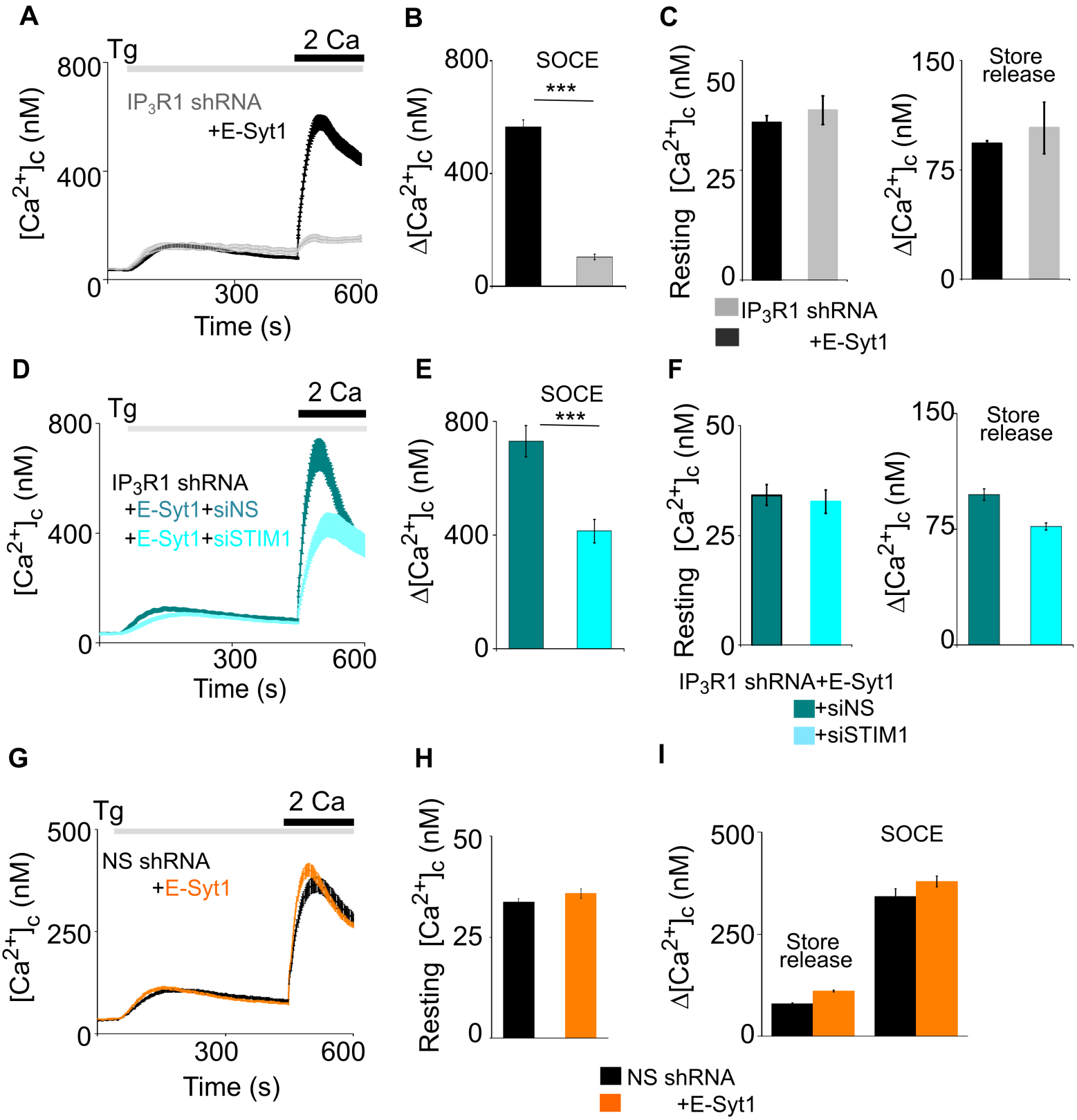
A
Tg
2 Ca
IP3R1 shRNA
+E-Syt1
[Ca2+]c (nM)
800
400
0
300
600
Time (s)
B
SOCE
***
Δ[Ca2+]c (nM)
800
400
0
C
Resting [Ca2+]c (nM)
50
25
0
Store release
150
75
0
IP3R1 shRNA
+E-Syt1
D
Tg
2 Ca
IP3R1 shRNA
+E-Syt1+siNS
+E-Syt1+siSTIM1
[Ca2+]c (nM)
800
400
0
300
600
Time (s)
E
SOCE
***
Δ[Ca2+]c (nM)
800
400
0
F
Resting [Ca2+]c (nM)
50
25
0
Store release
150
75
0
IP3R1 shRNA+E-Syt1
+siNS
+siSTIM1
G
Tg
2 Ca
NS shRNA
+E-Syt1
[Ca2+]c (nM)
500
250
0
300
600
Time (s)
H
Resting [Ca2+]c (nM)
50
25
0
I
SOCE
Store release
Δ[Ca2+]c (nM)
500
250
0
NS shRNA
+E-Syt1

Figure 8

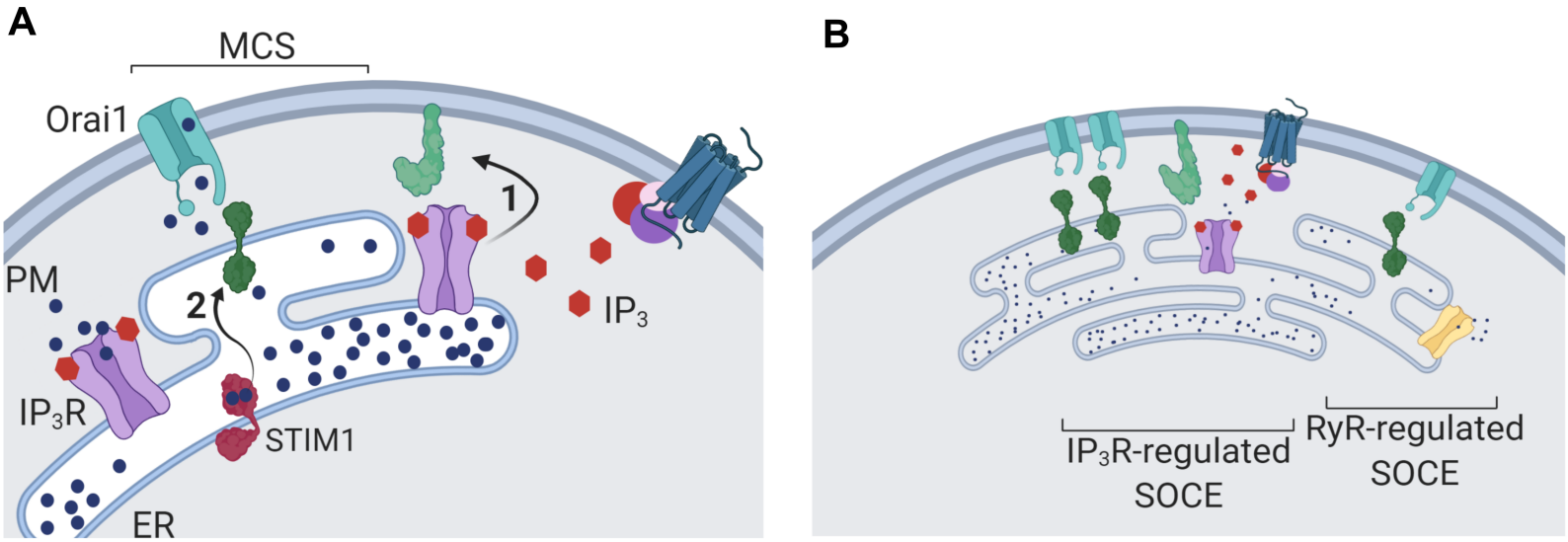
A
MCS
Orai1
PM
1
2
IP3
IP3R
STIM1
ER
B
IP3R-regulated
SOCE
RyR-regulated
SOCE

Figure 1- figure supplement 1

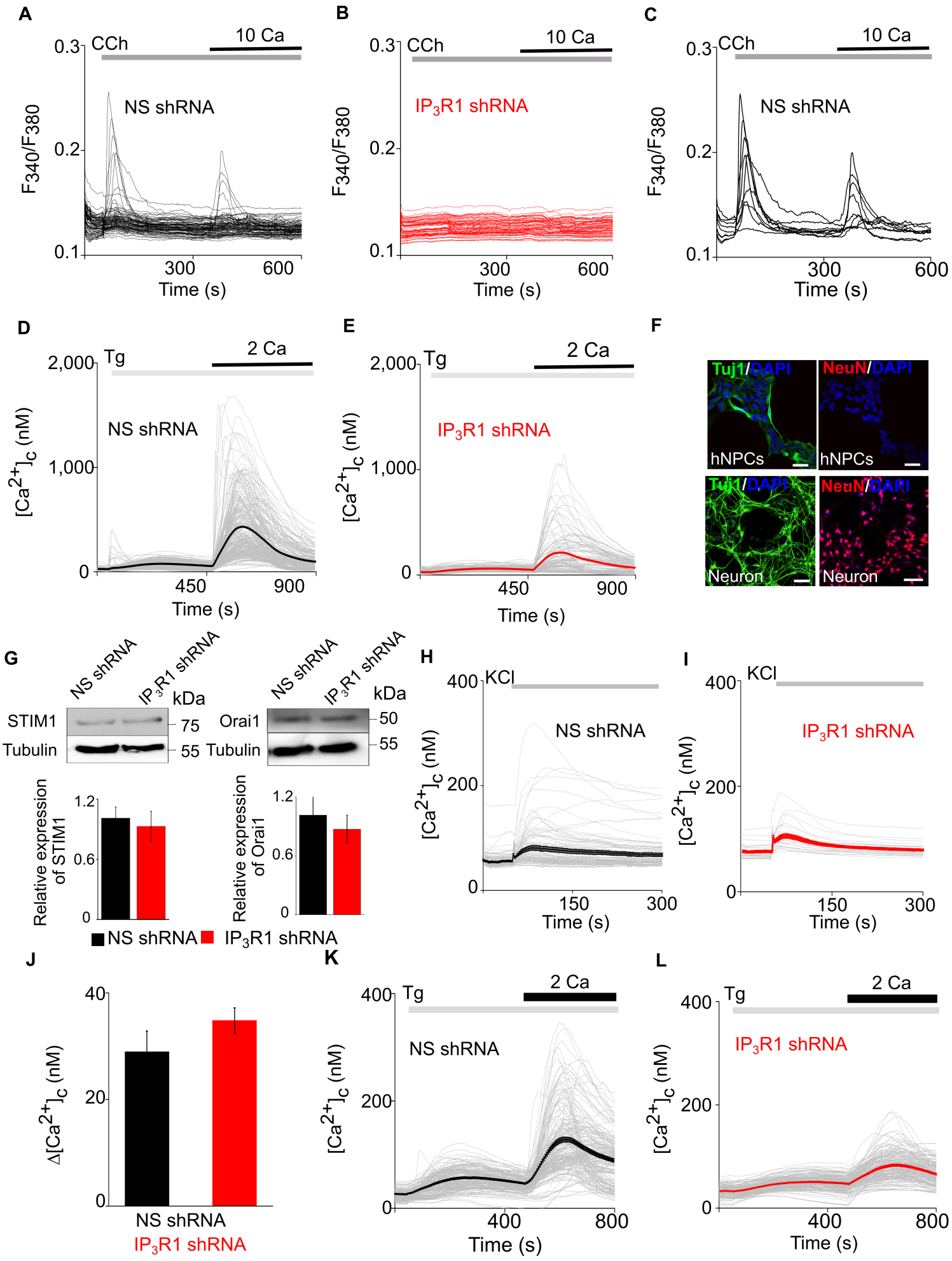

Figure 2- figure supplement 1

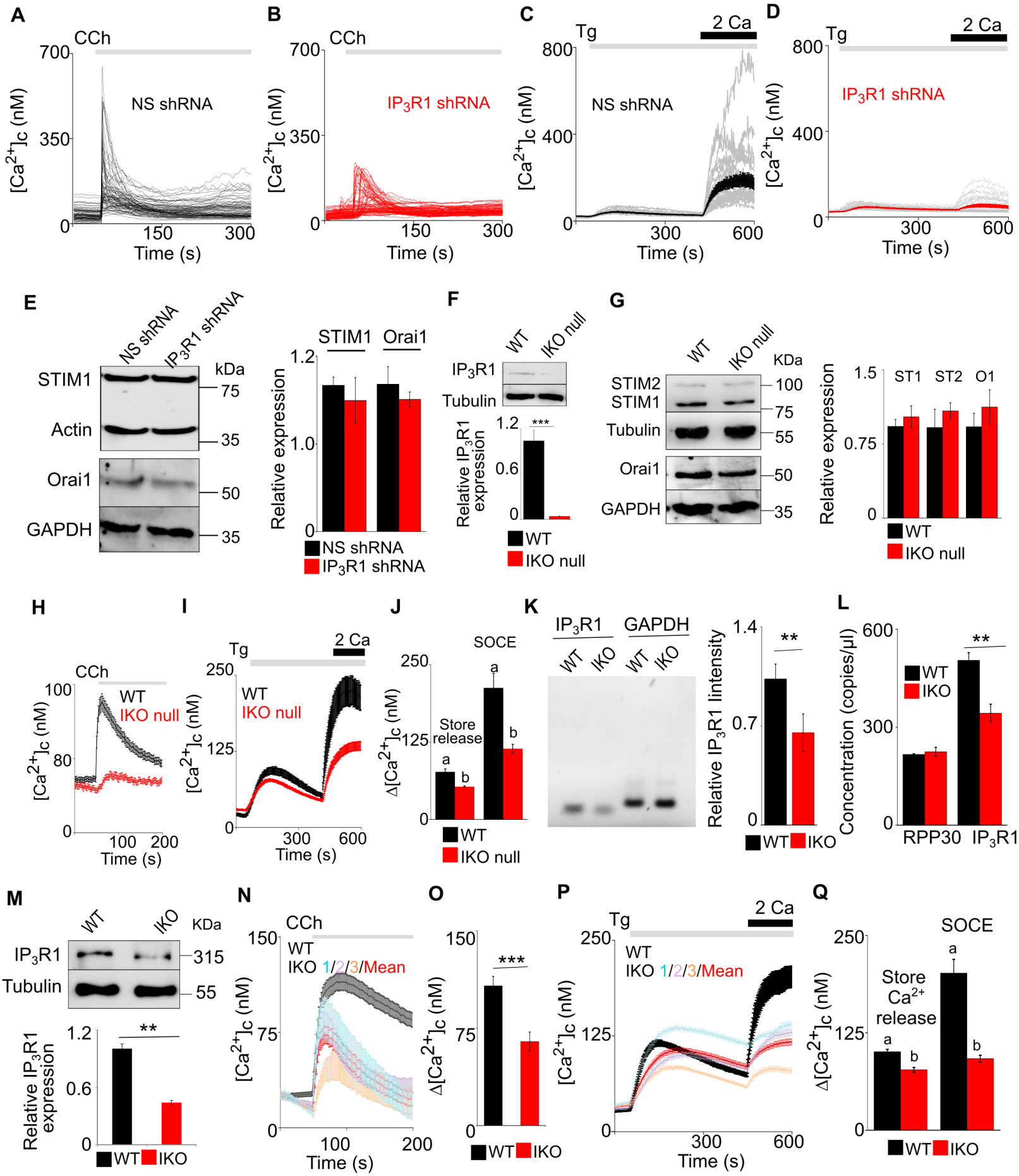

Figure 2- figure supplement 2

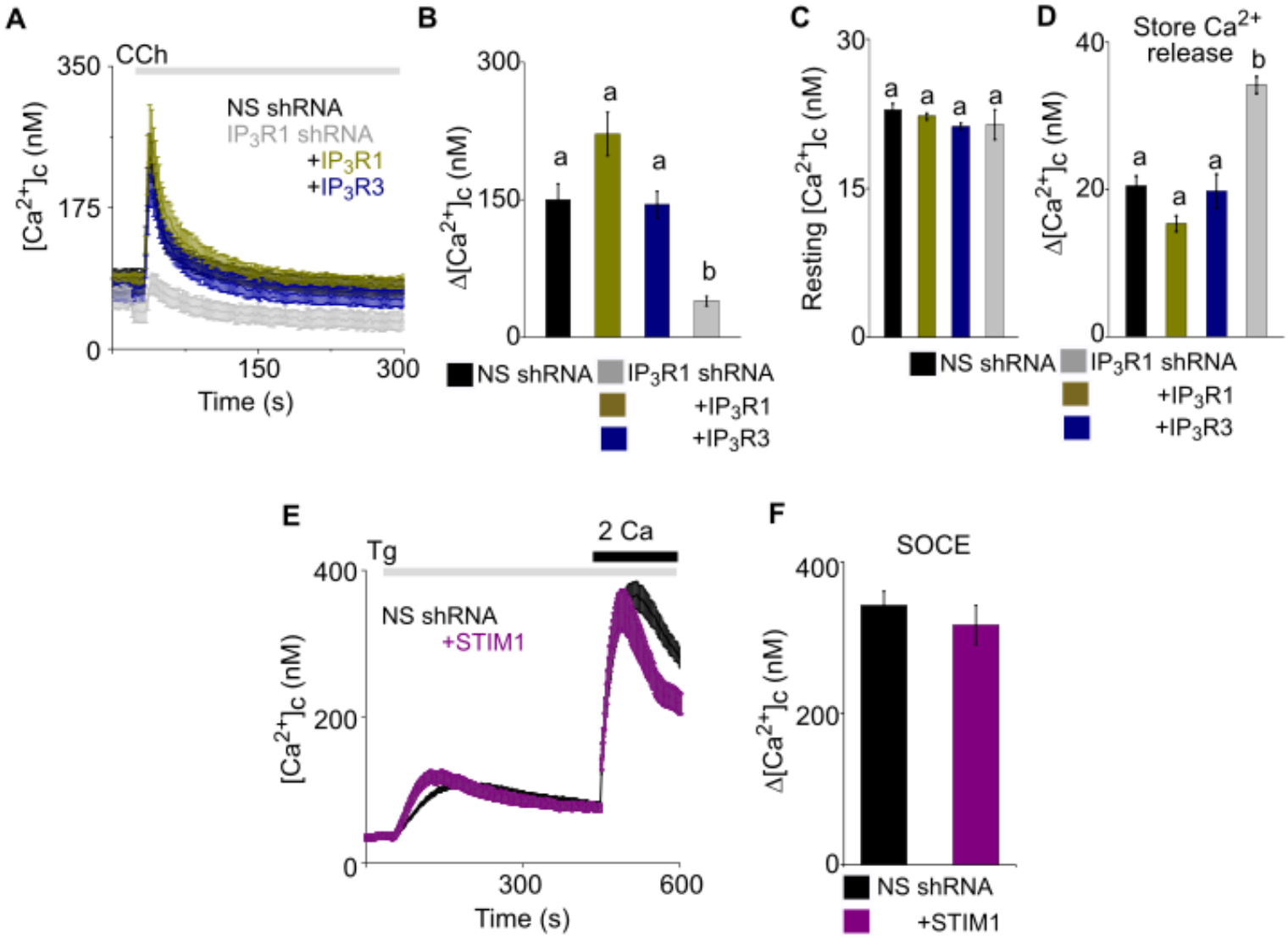

Figure 2- figure supplement 3

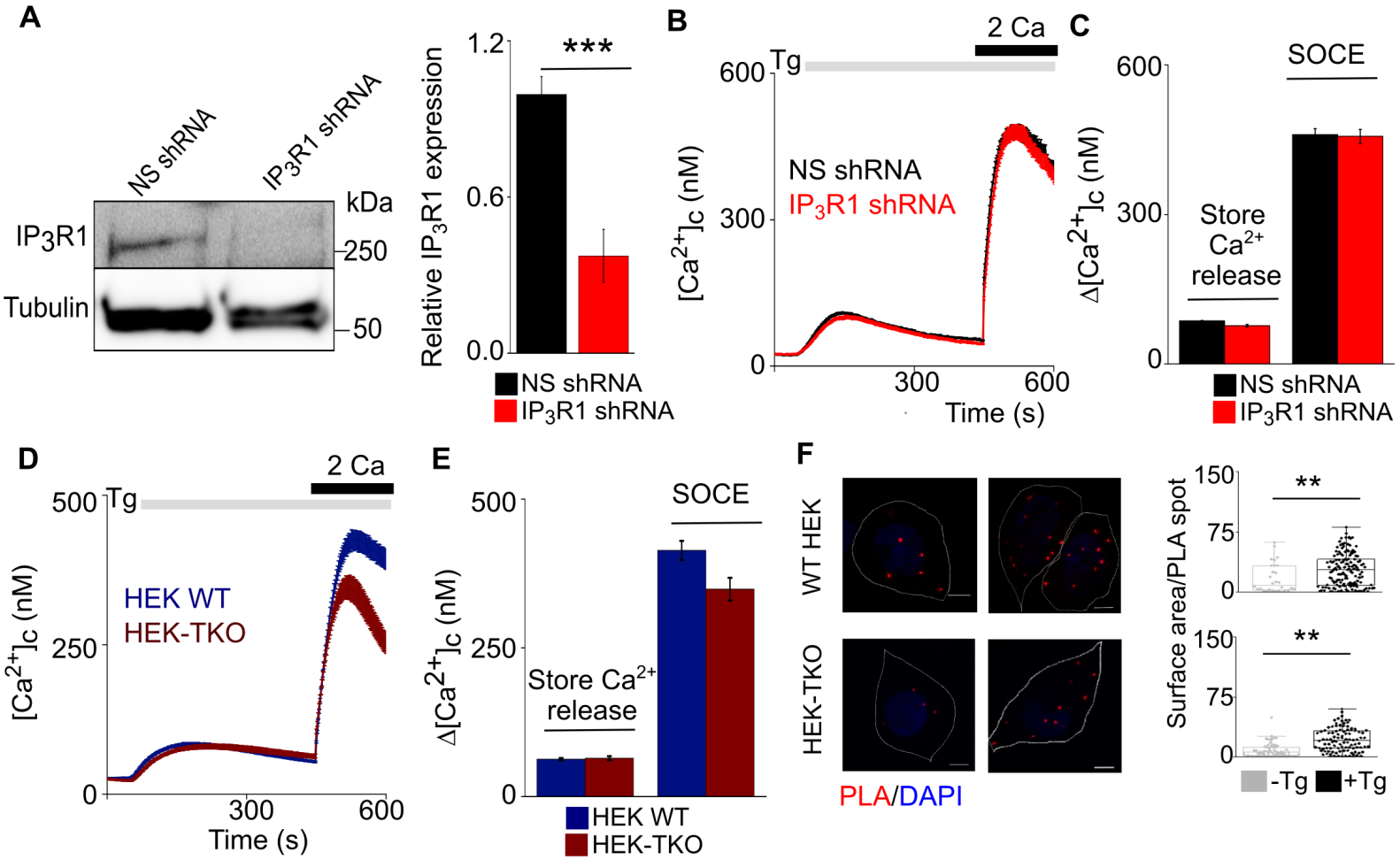

Figure 3- figure supplement 1

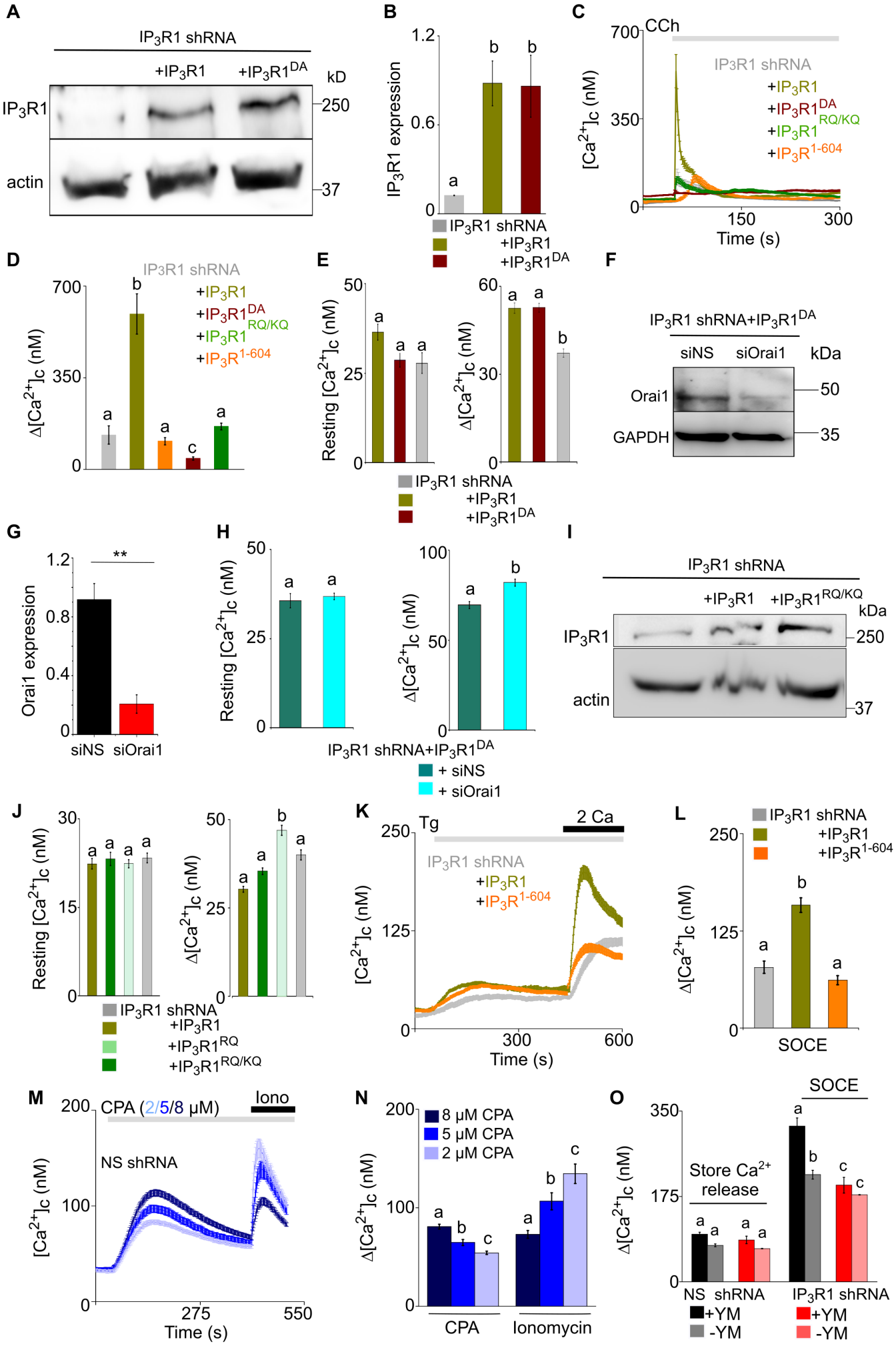

Figure 4- figure supplement 1

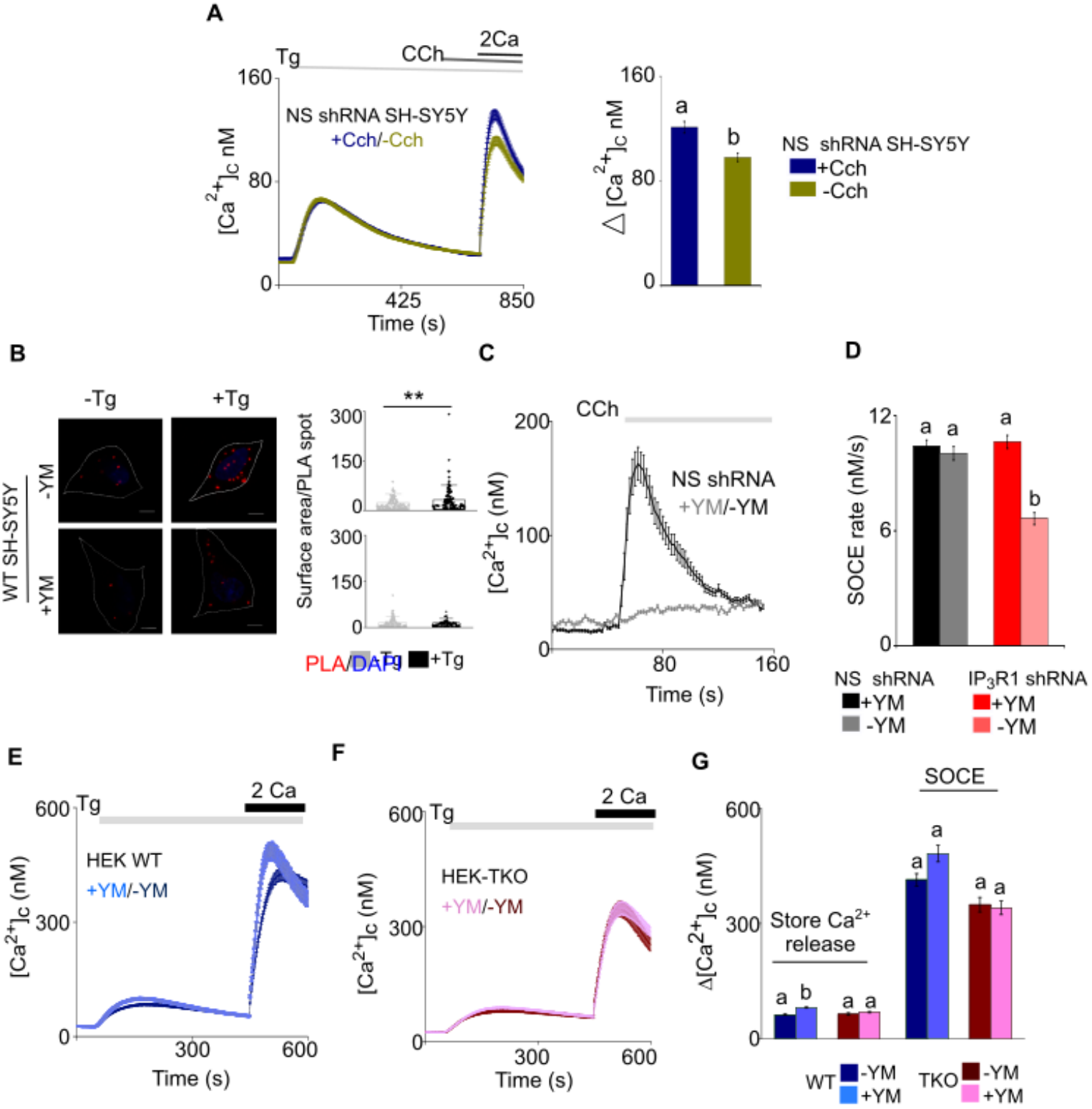

Figure 5- figure supplement 1

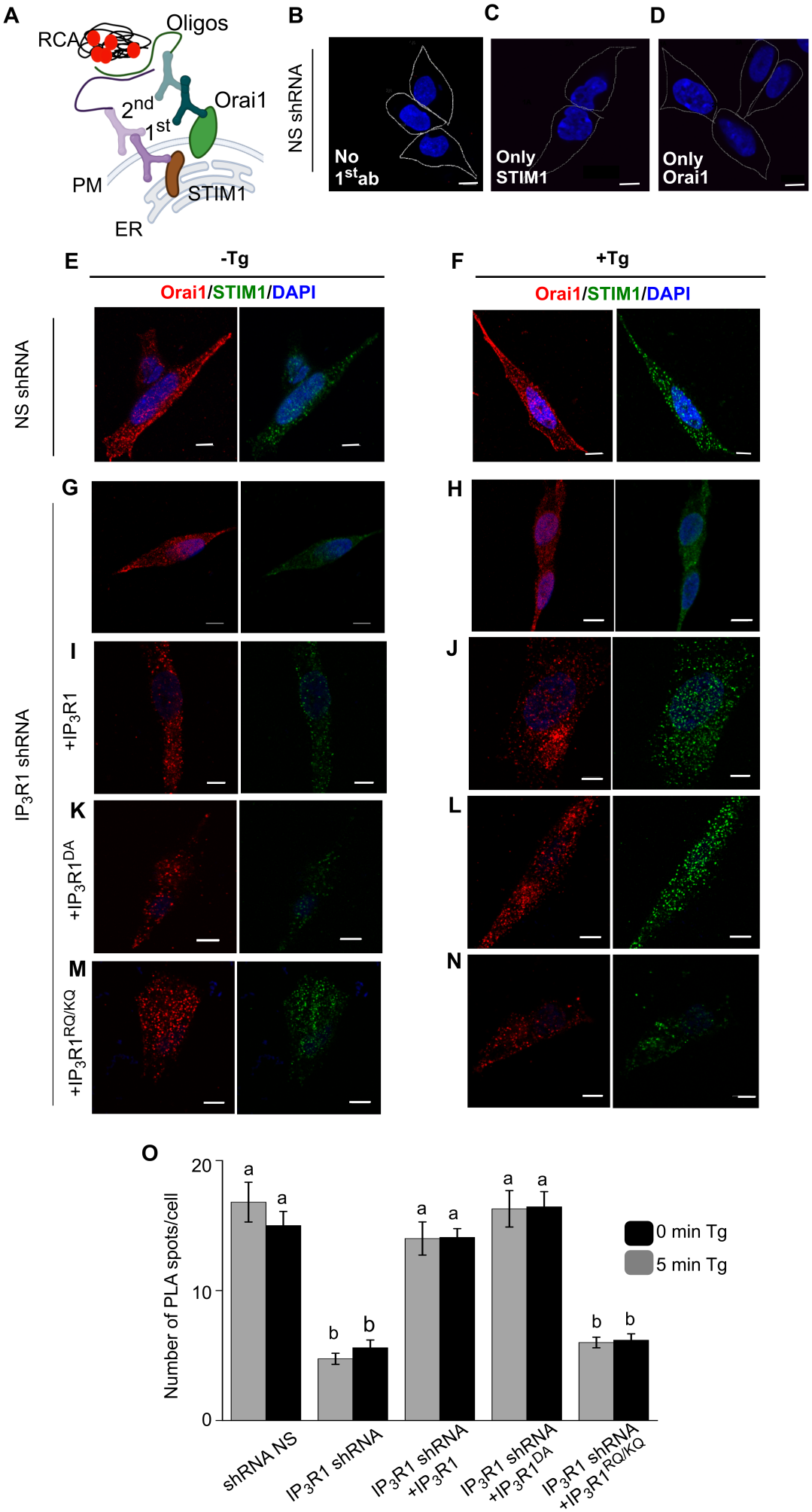
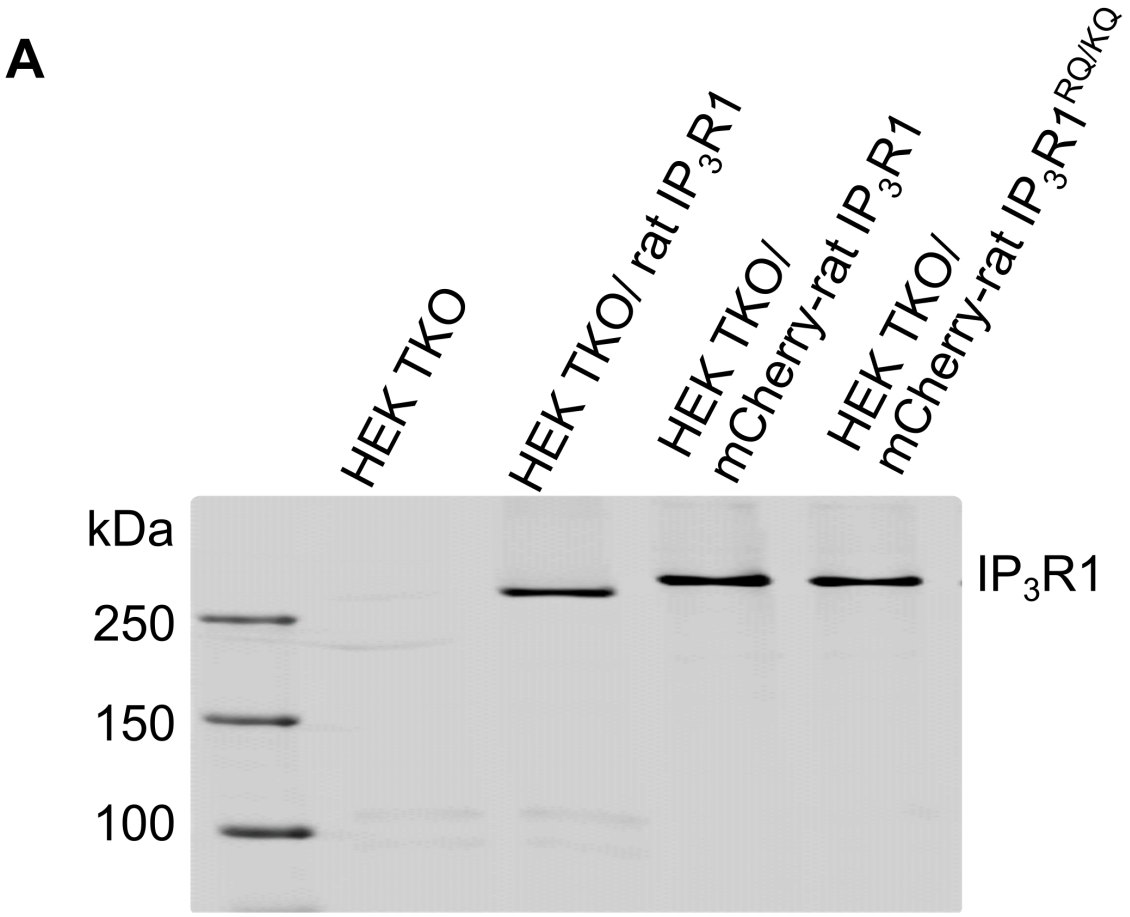
Figure 6- figure supplement 1